2000-08

The Arctic Ocean Response to the North Atlantic Oscillation

Dickson, R.R.

Journal of Climate, Volume 13, pp. 2671-2696.
http://hdl.handle.net/10945/45716

The Arctic Ocean Response to the North Atlantic Oscillation

R. R. DICKSON,* T. J. OSBORN,+ J. W. HURRELL,# J. MEINCKE,@ J. BLINDHEIM,& B. ADLANDSVIK,& T. VINJE,** G. ALEKSEEV,++ AND W. MASLOWSKI##

* *Centre for Environment, Fisheries and Aquaculture Science, Lowestoft Laboratory, Suffolk, United Kingdom*
+ *Climatic Research Unit, School of Environmental Sciences, University of East Anglia, Norwich, Norfolk, United Kingdom*
# *Climate and Global Dynamics, National Center for Atmospheric Research, Boulder, Colorado*
@ *Institüt fur Meereskunde, Universität Hamburg, Hamburg, Germany*
& *Institute for Marine Research, Bergen, Norway*
** *Norwegian Polar Institute, Oslo, Norway*
++ *Arctic and Antarctic Research Institute, St. Petersburg, Russia*
Oceanography Department, Naval Postgraduate School, Monterey, California

(Manuscript received 26 May 1998, in final form 28 July 1999)

ABSTRACT

The climatically sensitive zone of the Arctic Ocean lies squarely within the domain of the North Atlantic oscillation (NAO), one of the most robust recurrent modes of atmospheric behavior. However, the specific response of the Arctic to annual and longer-period changes in the NAO is not well understood. Here that response is investigated using a wide range of datasets, but concentrating on the winter season when the forcing is maximal and on the postwar period, which includes the most comprehensive instrumental record. This period also contains the largest recorded low-frequency change in NAO activity—from its most persistent and extreme low index phase in the 1960s to its most persistent and extreme high index phase in the late 1980s/early 1990s. This long-period shift between contrasting NAO extrema was accompanied, among other changes, by an intensifying storm track through the Nordic Seas, a radical increase in the atmospheric moisture flux convergence and winter precipitation in this sector, an increase in the amount and temperature of the Atlantic water inflow to the Arctic Ocean via both inflow branches (Barents Sea Throughflow and West Spitsbergen Current), a decrease in the late-winter extent of sea ice throughout the European subarctic, and (temporarily at least) an increase in the annual volume flux of ice from the Fram Strait.

1. Introduction

a. Characteristics of the NAO

The North Atlantic oscillation (NAO) is a large-scale alternation of atmospheric mass with centers of action near the Icelandic low and the Azores high. It is the dominant mode of atmospheric behavior in the North Atlantic sector throughout the year, although it is most pronounced during winter and accounts for more than one-third of the total variance in sea level pressure (SLP; Fig. 1a). The NAO alternates between a ''high-index'' pattern, characterized by an intense Iceland low with a strong Azores ridge to its south and a ''low-index'' pattern in which the signs of these anomaly cells are approximately reversed. The pressure difference between these two main cells is the conventional index of NAO activity. Here, we use the winter (December–March, hereinafter DJFM) index of Hurrell (1995a, 1996), which is based on the difference between normalized pressures at Lisbon, Portugal, and Stykkisholmur, Iceland.

Recently, Thompson and Wallace (1998, 2000; Thompson et al. 2000) suggested that the NAO may be the regional manifestation of an annular (zonally symmetric) hemispheric mode of variability characterized by a seesaw of atmospheric mass between the polar cap and the middle latitudes in both the Atlantic and Pacific Ocean basins. A very similar structure is also evident in the Southern Hemisphere. They named this mode the Arctic Oscillation (AO) and showed that, during winter, its vertical structure extends deep into the stratosphere. Similar findings have previously been recognized in the context of tropospheric–stratospheric coupling (Baldwin et al. 1994; Perlwitz and Graf 1995; Cheng and Dunkerton 1995; Kitoh et al. 1996; Kodera et al. 1996).

The NAO and the AO are nearly indistinguishable in the time domain: the correlation coefficient of monthly anomalies over the Northern Hemisphere cold season (November–April) is 0.95 (Deser 2000). This comes about because of the dominance of the Atlantic–Arctic

Corresponding author address: Dr. Robert Dickson, The Center for Environment, Fisheries and Aquaculture Science, Lowestoft Laboratory, Pakefield Rd., Lowestoft, Suffolk NR33 OHT, United Kingdom.
E-mail: r.r.dickson@cefas.co.uk

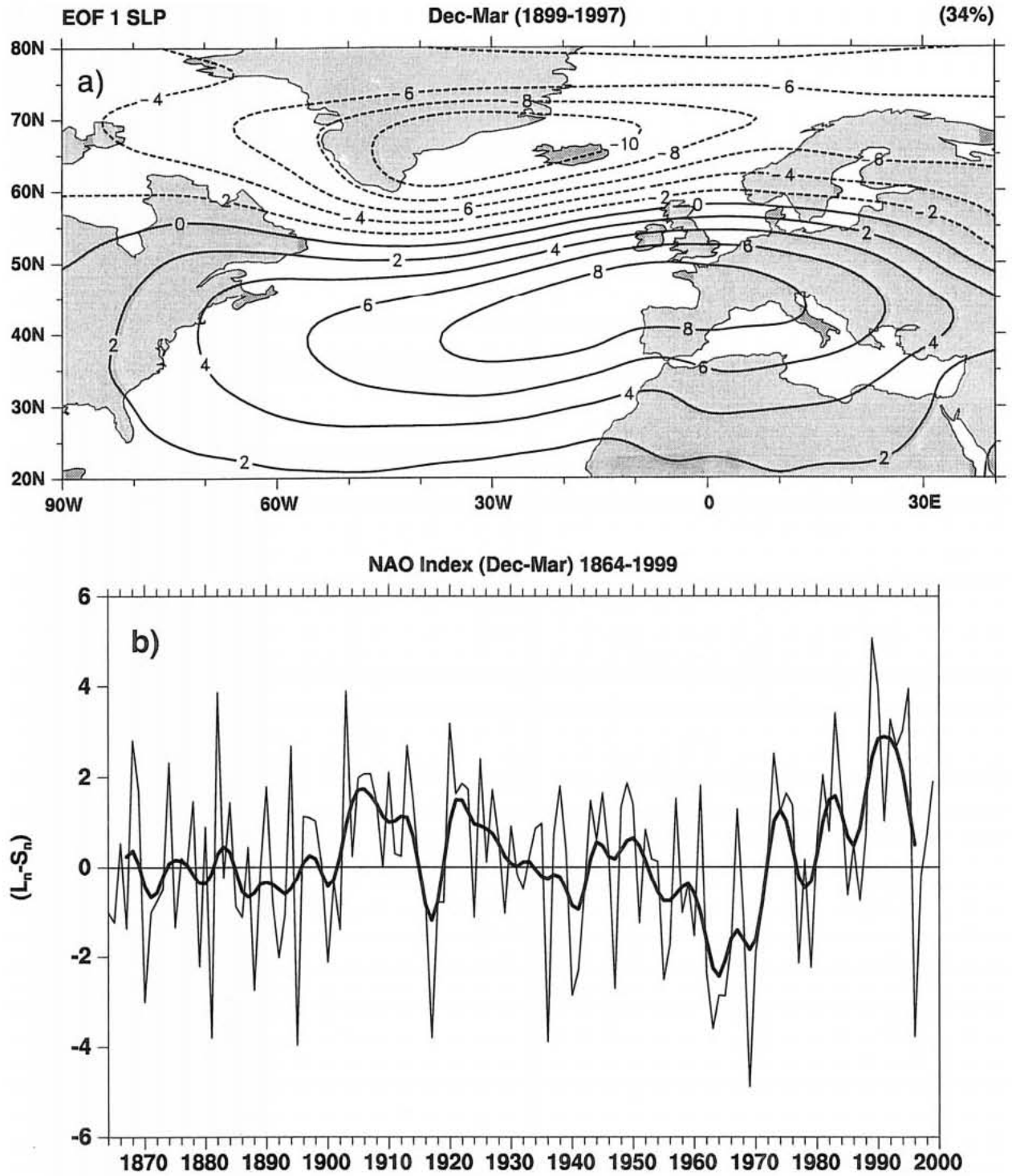

FIG. 1. (a) The first EOF of winter SLP for the North Atlantic sector based on Trenberth and Paolino (1980), and created from DJFM means over the period 1899–1977. The EOF is based on the covariance matrix and explains 34% of the variance. (b) The winter (DJFM) NAO index, updated from Hurrell (1995a).

sector on the AO. Indeed, there exists only a very weak association between the Atlantic and Pacific components of the AO (Hurrell 1996; Deser 2000). The signature of the AO on local temperatures and precipitation is, therefore, essentially the same as that of the NAO [e.g., compare Figs. 1 and 2 of Thompson et al. (2000) to Figs. 3 and 4 of Hurrell (1995a)]. Because the NAO and AO have much more in common than they have differences, here we focus on the longer NAO record.

The NAO index exhibits considerable long-term variability. Cook et al. (1998) and Hurrell and van Loon (1997) describe concentrations of spectral power around periods of 24, 8, and 2.1 yr, but also identify a multidecadal signal that appears to be amplifying with time. Thus the 1960s exhibited the most extreme negative phase of the index, the late 1980s/early 1990s experienced its most prolonged positive phase, and the change from the low-index 1960s to the high-index 1990s became the largest low-frequency change of record [Fig. 1b, updated from Hurrell (1995a)]. The extreme nature of NAO behavior has continued into the most recent years. Not only have 17 of the past 20 winters, including winter 1999, been NAO positive, but this period also included one of the largest year-on-year changes of record as the long positive sequence of the 1990s was interrupted by the third-lowest value of the century in winter 1996.

These changes have been associated with a wide range of physical and biological responses in the North Atlantic. These include variations in wind speed; latent and sensible heat flux; (Cayan 1992a,b,c), evaporation–precipitation (Cayan and Reverdin 1994; Hurrell 1995a); the distribution, prevalence, and intensity of Atlantic storms (Rogers 1990, 1994, 1997; Hurrell 1995b; Alexandersson 1998; WASA Group 1997), and hence effects on the wave climate (Bacon and Carter 1993; Kushnir et al. 1997; WASA Group 1997; Cotton and Challenor 1999; Carter 1999); sea surface temperature (Cayan 1992c; Hansen and Bezdek 1996); the strength of the Labrador Current (Myers et al. 1989; Marsh et al. 1999); the characteristics and distribution of water masses (Lazier 1995; McCartney et al. 1996; McCartney et al. 1997; Joyce and Robbins 1996; Houghton 1996; Molinari et al. 1997; Sy et al. 1997; Joyce et al. 1999; Curry et al. 1998; Curry and McCartney 2000, manuscript submitted to *J. Phys. Oceanogr.*); the extent of the marginal ice zone (Fang and Wallace 1994; Mysak et al. 1996; Deser et al. 2000); Davis Strait ice volume (Deser and Blackmon 1993); the iceberg flux past Newfoundland [K. Drinkwater, in Rhines (1994)]; and the intensity of deep convection at the main Atlantic sites (Greenland, Labrador, and Sargasso Seas; Dickson et al. 1996; Talley 1996; Dickson 1997; Joyce et al. 2000). Effects on the marine ecosystem include changes in the production of zooplankton (Fromentin and Planque 1996), the distribution of Atlantic salmon (Friedland et al. 1993; Dickson and Turrell 1999), and the recruitment of cod (Planque and Fox 1998).

In general terms, we are aware of certain general linkages between the NAO, the Arctic, and global change, though the specific response of the Arctic Ocean to these changes is much less well known. This paper aims to identify and where possible to quantify the broadscale nature of that response, and even though we will not, finally, be able to answer them, the following two questions form a large part of our motivation in doing so:

- *To what extent does the extension of the warm Atlantic Water layer in the Arctic Ocean during the late 1980s and early 1990s reflect the involvement of the NAO?* The first modern trans-Arctic CTD-tracer section worked by Canadian and U.S. icebreakers in 1993–94 and the Science Ice Expeditions (SCICEX) series of submarine surveys have revealed spectacular interannual changes in the temperature and salinity field of the Eurasian Basin at near-surface depths. By 1993, Atlantic layer temperatures had risen by 1°–2°C over the Lomonosov Ridge, and the extent of the warmest Atlantic-derived waters had clearly broadened (Quadfasel et al. 1991; Carmack et al. 1995; Aagaard et al. 1996; Swift et al. 1997; Carmack et al. 1997; Morison et al. 1998a,b; Morison et al. 2000; McLaughlan et al. 1996; Kolatschek et al. 1996)]. Around that time, the NAO was at its record positive phase (Hurrell 1995a; Jones et al. 1997).
- *To what extent does the NAO control the export of ice and freshwater from the Arctic to the open Atlantic?* With other more localized effects farther south, this flux is thought to promote significant changes in the ''headwaters'' of the global thermohaline circulation. During the extreme NAO low-index conditions of the 1960s, an extra 2000 km^3 of ice and freshwater were brought south from the Arctic Ocean in a swollen East Greenland Current (Dickson et al. 1988; Aagaard and Carmack 1989), but as great or greater changes have been measured in the volume flux of ice from Fram Strait during the 1990s.

b. Selection of NAO extrema

Throughout this paper, we concentrate on the winter season (December–February, hereinafter DJF), as the season of strongest forcing, and on the postwar years, 1947–96, as the period of best data. This period includes both the extreme NAO minimum of the 1960s and the record NAO maximum of the 1990s. The Lisbon–Iceland index is used rather than the Azores–Iceland version because of its marginally higher signal-to-noise ratio in winter (Hurrell and van Loon 1997). Our results, however, are insensitive to the particular index used (Osborn et al. 2000). Much of the analysis is based on the comparison of composite fields representing NAO-plus (NAO+) and NAO-minus (NAO−) conditions, se-

lected by using all winter months or seasons that equal or exceed 1 standard deviation (std dev) from the 130-yr mean.

The above gives us the following 33 months for the NAO− composite:

- Decembers of 1950, 58, 61, 63, 68, 70, 76, 78, 81, 89, 95
- Januaries of 1955, 59, 63, 66, 69, 70, 77, 79, 85, 87, 96
- Februaries of 1947, 55, 56, 60, 63, 65, 66, 68, 69, 78, 86;

and the following 28 months for the NAO+ composite:

- Decembers of 1951, 56, 72, 74, 79, 80, 82, 86, 88, 93, 94,
- Januaries of 1957, 74, 83, 84, 89, 90, 93, 95,
- Februaries of 1949, 50, 59, 61, 82, 89, 90, 92, 95.

Where appropriate, we compare parameters on composites of extreme winter seasons. Defining the winter by the year of the January, the dataset yields the following 11 seasons for the NAO− composite:

- winters (DJF) of 1947, 55, 56, 63, 64, 65, 66, 69, 77, 79, 96

and the following 11 seasons for the NAO+ composite:

- winters (DJF) of 1949, 73, 75, 81, 83, 84, 89, 90, 92, 93, 95

Last we selected a consecutive sequence of NAO-extreme years, for the comparison of cases where a process (e.g., circulation modeling) is continuously evolving, where the ocean's response is buffered or where the data impose a lower time resolution. These sequences were:

- the NAO− 7-yr run: winters 1963–69 inclusive
- the NAO+ 7-yr run: winters 1989–95 inclusive.

In both sets, five out of the seven are >1 std dev from the mean, two of which are >2 std devs from the mean.

c. Mean sea level pressure (MSLP)

Three main datasets are available for the task of compiling NAO+ and NAO− composites of mean sea level pressure for the Arctic and Subarctic. The degree of data overlap between these sets is unclear, and all three were examined in compiling this most basic set of composites. The U.K. Met Office (UKMO; Jones 1987, updated) and the National Center for Atmospheric Research (NCAR; Trenberth and Paolino 1980, updated) datasets are both operational analyses of rather coarse resolution ($10° \times 5°$ grid and 350 km, respectively) but of century-long duration. The most reliable period is from the 1960s to date in view of earlier assumptions about a ''polar high'' (Jones 1987). The third dataset derives from the International Arctic Buoy Program (WMO 1994), and provides a gridded dataset for the central Arctic at finer resolution ($2° \times 10°$) but shorter duration (post 1979) than the above.

Two other data sources were also considered but not used. European Centre for Medium-Range Weather Forecasts (ECMWF) and National Centers for Environmental Prediction (NCEP) reanalyses provide finer resolution but, at the time of writing, were of shorter duration than the operational sets (1979 and 1972, respectively); direct observations of winds at a cluster of Russian north polar stations are now available on CD-ROM for most years 1950–91 (Environmental Working Group 1997) but proved to be of variable extent and data density. (Note that prior to 1979, the density of Arctic observations is probably low in all datasets relative to the more densely observed latitudes in which the NAO has been studied previously.)

The composite winter MSLP distributions at NAO positive and negative extrema proved to be similar in each of the main datasets and are described using the UKMO set in Fig. 2. In Figs. 2a–d we show these composites as distributions of absolute winter SLP and of SLP anomaly, respectively, together with the difference in SLP anomaly distribution from low index to high (Fig. 2e).

Winter months with a high NAO index (Fig. 2a) show an intense low pressure cell centered over the Irminger Sea, while low-index winter months show a much weakened Iceland Low shifted to a position south of Greenland, and with a secondary low over the Barents Sea (Fig. 2b). The differences between these pressure patterns and the long-term mean winter SLP reveal anomaly patterns that are almost identical to one another, though of opposite sign (Figs. 2c,d). In each, the largest anomaly is in the vicinity of Iceland, but pressure changes of the same sign (decreases for high NAO, increases for low NAO) extend over the entire Arctic Ocean. Thus as low-index conditions give way to high, the overall pressure change at Iceland amounts to -22 mb, decreasing in amplitude northward across the Arctic Ocean to a line of zero change near the Bering Strait.

d. Pattern dominance, NAO versus NP

To check for possible Pacific influences on Arctic climate, the UKMO operational dataset was used to provide MSLP composites at extreme states of the North Pacific index (NP; Trenberth and Hurrell 1994) over the same period. The NP index is closely correlated ($r = 0.93$) with the Pacific–North America pattern. Defining the NAO and NP ''signal strength'' to be the absolute pressure difference between their high- and low-index composites, we can use the ratio of these signal strengths to describe their respective areas of dominance. Figure 3 confirms that values of this ratio of two or more (NAO signal strength twice that of NP), cover much of the Arctic and Nordic Seas, whereas values less than 0.5 (NP signal strength twice that of NAO) are confined south of the Bering Strait. Deser (2000) has also shown

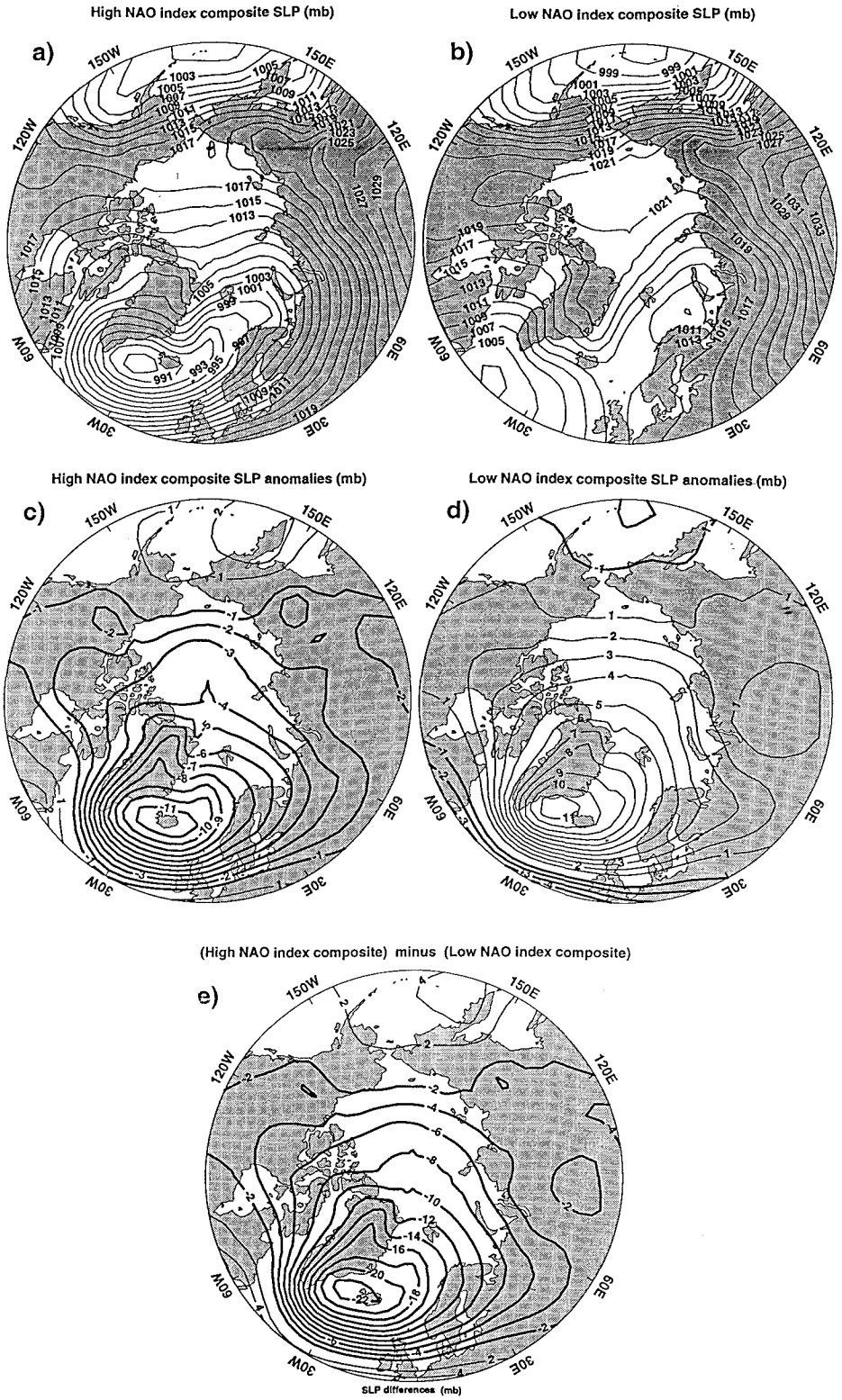

FIG. 2. Distributions of (a), (b) winter SLP and (c), (d) SLP anomaly for composites of winter months representing high-index and low-index states of the NAO. (e) The change in SLP from the low-index composite to the high.

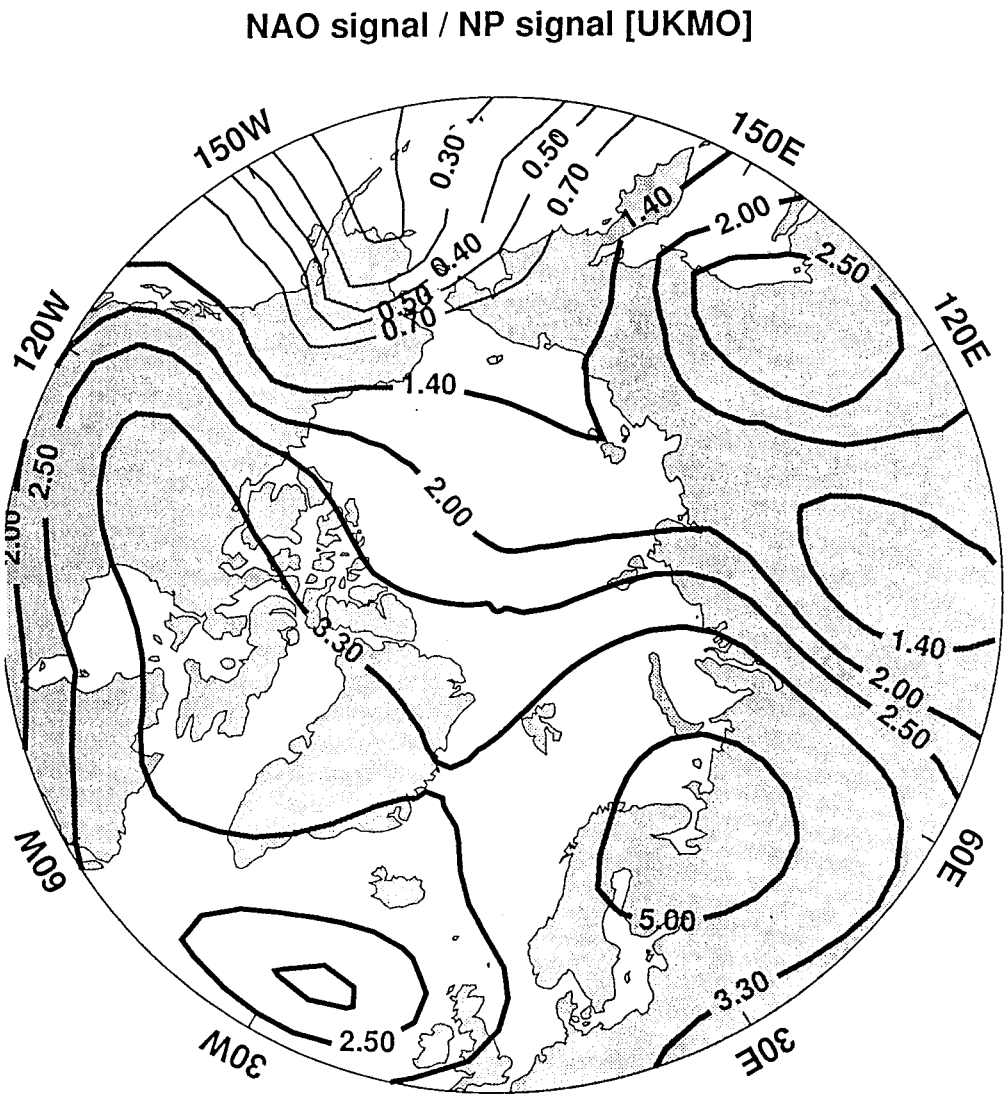

FIG. 3. Ratio of the winter ''signal strengths'' of NAO and NP modes of atmospheric behavior across the Arctic and subarctic. The ''signal strength'' of each mode is defined as the absolute pressure difference (mb) between their high- and low-index composites, selected using all winter (DJF) months that equal or exceed 1 std dev from the long-term mean value of that index. Ratios of 2 or more (NAO signal strength twice that of NP) cover much of the Arctic, whereas values less than 0.5 (NP signal strength twice that of the NAO) are confined to south of the Bering Strait.

that SLP variability over the Pacific is only weakly associated with pressure variations over the Arctic, while the Atlantic and the Arctic are strongly coupled. We conclude from these results that surface pressure variations over the Pacific, relative to those over the Atlantic, have a relatively small influence on the Arctic.

e. Storm climate

It is already well established that the NAO exerts a significant control on the track, prevalence, and intensity of Atlantic storms (Rogers 1990, 1994, 1997; Hurrell 1995b; Alexandersson et al. 1998; WASA Group 1997). Figures 4a,b, for example, describe the close relationship between the winter NAO index and the number of Atlantic winter storms deeper than 950 hPa (R. Francke 1998, personal communication), and Rogers describes the accompanying changes in storm distribution. The center of storm activity retracts southwestward to the American coast during the negative phase of the NAO (at which time very few deep storms are found anywhere in the Atlantic), but extends northeastward into the Norwegian–Greenland Seas during the opposite high-index phase accompanied by a remarkable increase in the incidence of deep storms to around 15 per winter.

More recent studies have quantified the change in

storm climate northward into the Arctic Ocean. Serreze et al. (1997) apply an automated cyclone detection and tracking algorithm to twice-daily National Meteorological Center (now known as NCEP) SLP fields over the period 1966–93 (i.e., covering much of the change from low- to high-index NAO activity) to describe a general increase in cold-season cyclone frequency over this period in the region north of 60°N (Fig. 4e). Using the same automated system, Maslanik et al. (1996) confirm that a similar sharp increase in cyclone frequency has taken place over the Arctic north of 75°N, between 60°E and 160°E (Fig. 4d); this in turn is in keeping with the conclusion of Walsh et al. (1996) that mean sea level pressures over the central Arctic have decreased between 1979–86 and 1987–94 in every calendar month (Fig. 4c), but with the largest and most significant reductions in autumn and winter. However, although the individual panels of Fig. 4 appear to show a certain commonality of change—most notably an increase in cyclone activity at mid- to high latitudes in the late 1980s and early 1990s—it would be wrong or oversimplistic to ascribe them all to the NAO and its changes. Certainly, the positive-minus-negative NAO difference field of cyclone activity for the cold season provided by Serreze et al. (1997, their Fig. 6) and the recent analysis by Rogers (1997) clearly link a stormier Atlantic in recent years with an increased cyclone prevalence in the Greenland, Iceland, Norwegian, and Barents Seas. But the former authors also point out that the recent increase in cyclone activity further to the north and east over the Kara Sea is the opposite to what would normally be expected under the positive phase of the NAO; and although a major decrease in pressure over the high Arctic *is* expected under these conditions. (cf. Figs. 2a,c), the pattern of the recent SLP change described by Walsh et al. is not simply that of the NAO. Thus the common features apparent in Figs. 4a,c,d,e may reflect some shared influence of the NAO on storms and the storm-track, but it is an influence that tapers off rapidly toward the high Arctic.

2. Inputs

a. Moisture flux

Serreze et al. (1995c) use an extensive rawinsonde archive (Kahl et al. 1992) to derive estimates of the meridional moisture flux across 70°N on a monthly timescale from 1974 to 1991, calculated for every 10° longitude, and integrated from the surface to 300 hPa. The period chosen reflects the increased vertical resolution for Eurasian stations after 1974, and the use of 70°N both utilizes the densest zonal coverage and allows comparison with the 1963–73 dataset of Piexoto and Oort (1992), albeit of lower resolution. They find that the integrated water vapor transport exhibits marked longitudinal variations, with a conspicuous maximum (25 kg m^{-1} s^{-1}) in the mean *annual* poleward transport near the prime meridian, presumed to be due to the high mean specific humidity at low levels and to its frequent advection northward by storms along this primary Atlantic cyclone track. The seasonality of the zonal-mean vapor flux is not conspicuous but peaks in September.

Beyond pointing out a range of potential climatic effects (that increased atmospheric moisture would tend to increase greenhouse warming, increase river runoff to the Arctic Ocean, affect sea-ice production and deep water formation in peripheral seas, and alter cloud cover), Serreze et al. do not address the interannual variability of poleward moisture flux. However, they have kindly provided their dataset for use in the present study.

Figure 5 describes the mean longitudinal distribution of moisture flux (kg m^{-1} s^{-1}) through 70°N in *winter* (DJF) 1974–91, together with curves illustrating the same quantity for composites of winter months at strongly positive and negative NAO extrema. Although the mean winter curve is essentially a lower amplitude version of the annual distribution (cf. Serreze et al. 1995c, their Fig. 8), the longitudinal distribution and especially the moisture flux through Nordic Seas become markedly different during extreme phases of the NAO. In the NAO+ composite, the peak moisture flux near the prime meridian doubles to 31 kg m^{-1} s^{-1}; during NAO− extrema, it dwindles there to near zero and instead shows its maximum poleward flux near the Davis Strait (≈60°W). This seems in line with what we know of the change in the Atlantic storm track during contrasting phases of the NAO. We have just described the extension of winter storm activity to the Norwegian–Greenland Sea during the high-index phase of the NAO; and Dickson and Namias (1976, their Fig. 7) confirm that the main winter storm track penetrated the Arctic along 60°W during the record negative NAO conditions of the 1960s.

Expressed as percentages of the total winter moisture flux entering the Arctic through 70°N, we find that 58% of an increased total flux enters through the 10°W–50°E sector during NAO+ conditions compared with 39% in the long-term mean and 0% during NAO− conditions. As a result, the total passing this 60° sector 10°W–50°E during NAO+ conditions is as high as the flux that passes north through the whole 360° sector during low-index conditions.

Because (in keeping with the rest of this study) these results apply solely to winter, it is relevant to determine how important moisture flux changes are in winter as compared with the year as a whole. In absolute terms, they are relatively small, though in terms of variability they are large.

Specifically, the average winter (DJF) moisture flux is 16.3% of the average annual flux (very close to one-sixth of the total), compared with 18.2% in spring, 37.4% in summer, and 28.1% in fall. On the other hand, the interannual standard deviation of DJF total moisture flux into the Arctic is 36% of the interannual standard deviation of the annual totals. Also, the time series of DJF moisture flux correlates quite highly with the time

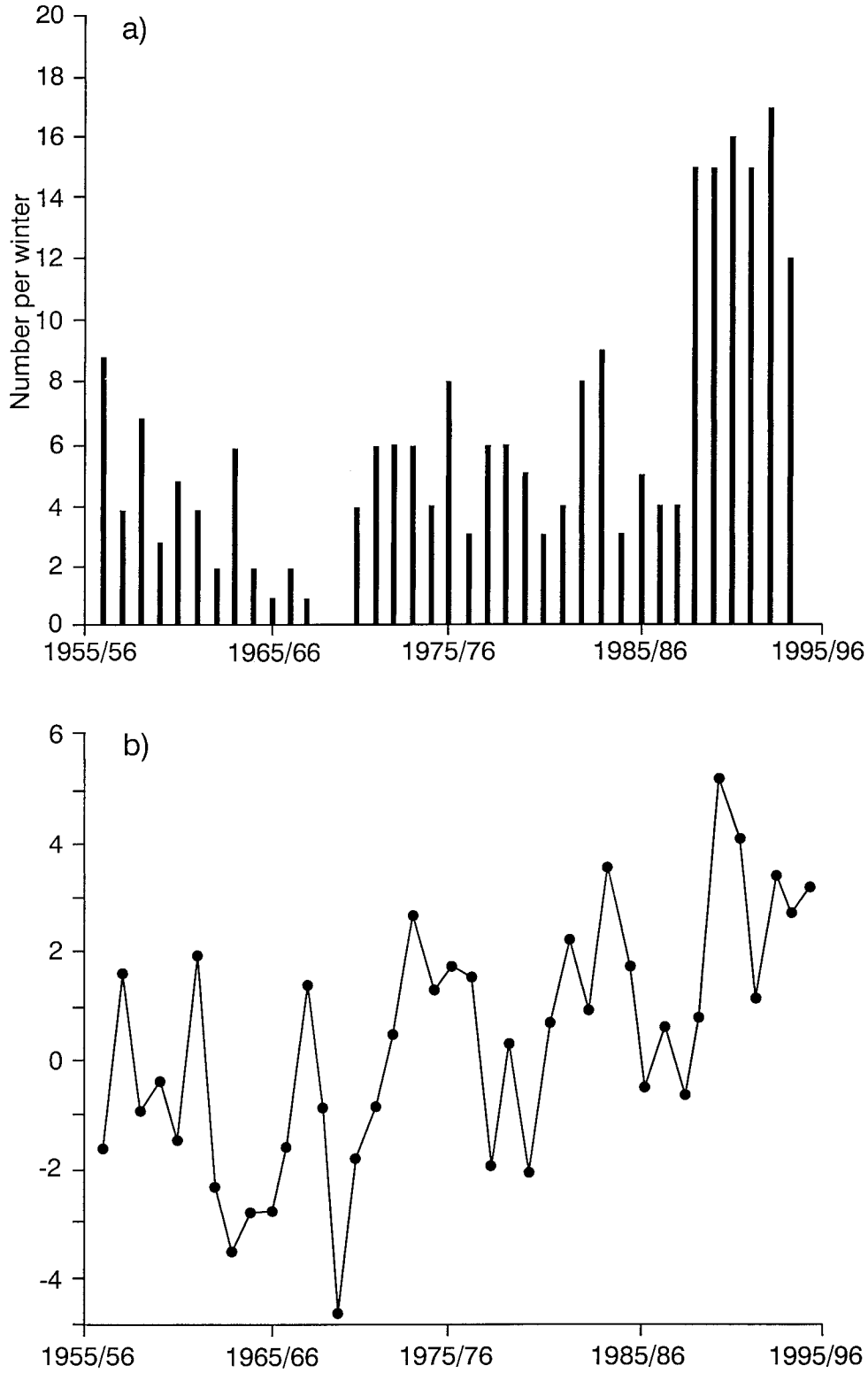

FIG. 4. Indices of storm activity at mid- to high latitudes. (a), (b) Number of Atlantic storms deeper than 950 hPa (R. Franke 1998, personal communication) compared with changes in the NAO index (Hurrell 1995a).

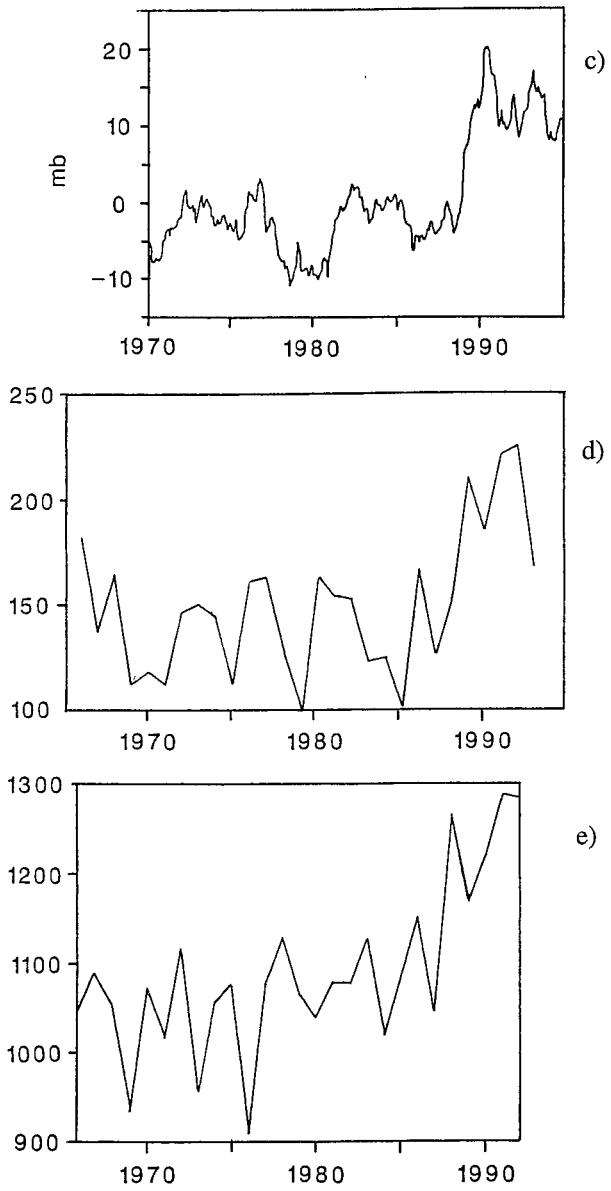

FIG. 4. (*Continued*) (c) Vorticity index for the central Arctic (from Walsh et al. 1996), (d) cold season cyclone count at 75°–90°N, 60°–160°E (from Maslanik et al. 1996), and (e) cold season cyclone count north of 60°N (from Serreze et al. 1997).

series of annual flux ($r = 0.73$ for DJF, compared to 0.45 for March–May, 0.78 for June–August, and 0.31 for September–November).

360° total moisture flux passing 70°N:

$$\text{NAO}+ = 7.55 \times 10^7 \text{ kg s}^{-1},$$

i.e., +28% cf. the long-term mean

$$\text{Mean} = 5.91 \times 10^7 \text{ kg s}^{-1}$$

$$\text{NAO}- = 4.36 \times 10^7 \text{ kg s}^{-1},$$

i.e., −26% cf. the long-term mean

Total moisture flux passing 70°N between 10°W and 50°E:

$$\text{NAO}+ = 4.35 \times 10^7 \text{ kg s}^{-1}$$

representing 58% of the 360° flux

$$\text{Mean} = 2.28 \times 10^7 \text{ kg s}^{-1}$$

representing 39% of the 360° flux

$$\text{NAO}- = -0.46 \times 10^7 \text{ kg s}^{-1}$$

representing 0% of the 360° flux

Figure 6 complements the above in showing the close correspondence between the time series of winter moisture flux convergence through 70°N and the winter NAO index (Hurrell 1995a). Because the dataset of Serreze et al. begins in 1974, the extreme low-index winters of the 1960s are not included. The NAO+ means and composites derived here are therefore much more representative than the NAO− values. We conclude from these relationships that the moisture flux to the Arctic is closely controlled by the NAO, acting via its general effect on the activity and intensity of the winter storm track through Nordic Seas.

b. Precipitation balance

Hurrell (1995a) used composited ECMWF analyses to show that at times of high NAO index, the axis of maximum moisture transport shifts to a more SW to NE orientation over the Atlantic and extends much farther to the north and east into northern Europe and Scandinavia. Hurrell and van Loon (1997) illustrate just such a pattern in showing (their Fig. 14) the change in precipitation corresponding to a unit deviation of the NAO index in winter during 1900–94. Since Hurrell's report, Xie and Arkin (1996) have greatly improved the data coverage, using station data blended with satellite products and (where neither exists) data from an assimilating model to provide global, gridded precipitation at 2.5° resolution for every month from 1979 to 1995. From this new dataset we compiled composites of mid to high-latitude precipitation for the following years:

- High-index NAO: 1983, 89, 90, 92, and 95
- Low-index NAO: 1979, 82, 85, 86, and 88

The high-index years are all above 1 std dev. However, starting in 1979, this dataset does not include the lowest-index years of the 1960s, and though all the low-index years shown are negative, only one (1979) is below 1 std dev. The difference in the distribution of precipitation between these two composites (Fig. 7) will therefore underestimate the precipitation change from low- to high-index conditions. Qualitatively, Fig. 7 agrees with Hurrell (1995b) in showing that the major precipitation increase (up to +15 cm per winter) during positive NAO conditions occurs in the "conduit" of the Norwegian–Greenland Seas and Scandinavia, presum-

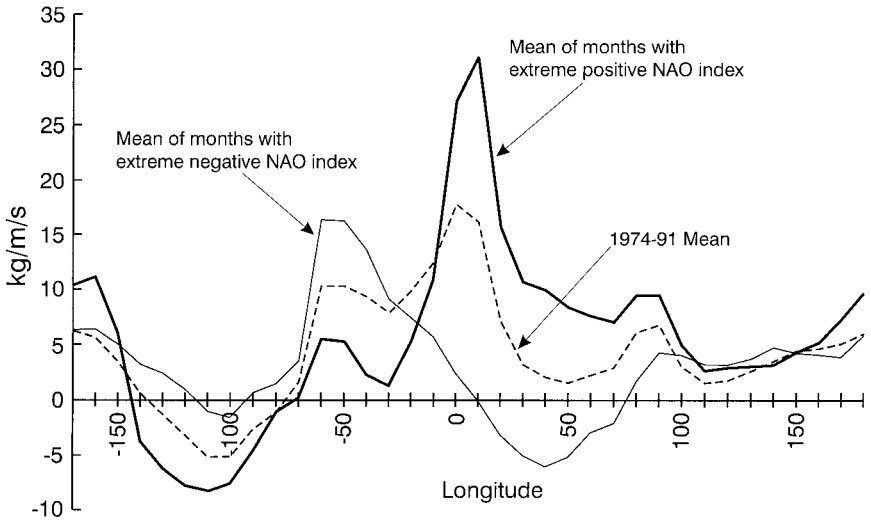

FIG. 5. Vertically integrated meridional moisture flux crossing 70°N in winter expressed as a function of longitude for composites of winter (DJF) months representing high-index and low-index NAO extrema. The 1974–91 winter mean is shown.

ably reflecting the changes in the Atlantic storm track already described; though there is a lesser response over the Arctic Ocean, it tends to be of the same sign (wet). [Note that Serreze et al. (1995a,b) find a 36% increase in climatological precipitation − evaporation ($P - E$) for the region north of 70°N in (high index) 1974–94 in comparison with that found by Piexoto and Oort (1992) for the preceding (low index) decade]. We cannot yet tell whether the cause of this major change in the precipitation balance of the subArctic and Arctic is natural or anthropogenic; we note merely that the coupled climate models of Manabe and Stouffer (1993, 1994) suggest roughly a 50% increase in high latitude $P - E$ for a world with doubled CO_2. The coupled model of Rahmstorf and Ganopolski (1999) also assigns a global importance to relatively minor changes in freshwater distribution at high latitudes.

c. Heat and Atlantic water flux

During the 1990s, there has been a major increase in the ship-based ocean-observing effort in the Arctic Ocean, contributed both by surface ships (*Polarstern* and *Oden* in 1987 and 1991, the first U.S./Canadian trans-arctic section in the summer of 1994 aboard *Polar Sea* and *Louis St. Laurent,* and three further *Polarstern* cruises in 1993, 1995, and 1996 were highlights), and by the almost-annual submarine surveys of the U.S. SCICEX Program (1993–99). Further, the release of a vast military archive of ocean data supplied an improved ocean ''climatology'' (Environmental Working Group 1997) against which the new datasets might be compared for evidence of change. The comparison revealed considerable differences in water mass characteristics, distribution, and exchange compared with earlier datasets, in particular a more intense and more widespread influence of Atlantic water than previously observed (Quadfasel et al. 1991; Carmack et al. 1995; Aagaard et al. 1996; Swift et al. 1997; Carmack et al. 1997; Morison et al. 1998a,b; Morison 2000; McLaughlan et al. 1996; Kolatschek et al. 1996).

Specifically, the Atlantic-derived sublayer in the Eurasian Basin (see Fig. 8 for locations) had warmed by 1°–2°C compared with Russian climatologies of the 1940s–70s (by 0.5°C since 1991 over the Lomonosov Ridge), its associated subsurface temperature maximum had shoaled (to ≈200 m in the SCICEX 1993 results), and the boundary between waters of Pacific and Atlantic origin had spread west from the Lomonosov to the vicinity of the Alpha–Mendeleev Ridge, extending the Atlantic water range by almost 20% (Morison et al. 1998a,b; Morison et al. 2000). Accompanying this change, Steele and Boyd (1998) reveal that the cold halocline layer, which acts to insulate the sea ice from the warm Atlantic layer below, had dwindled away in the Eurasian Basin with profound effects on the surface energy and mass balance of sea ice in that region. Hydrography, tracers, and modeling all suggest that this change stemmed from the eastward diversion of Russian river input in response to the altered atmospheric circulation (see Maslowski's model output, in Dickson 1999), and Arctic-wide, the whole pattern of atmospheric pressure and ice drift appears to have shifted counterclockwise in a similar sense.

Grotefendt et al. (1998) have analyzed the changes in the Atlantic water layer and cite four main contributory factors. They suspect that a part of the change—perhaps up to half in places—may be due to the poor vertical resolution and increased space–time smoothing of the old climatologies as compared with modern CTD data. However, where the warming is strongest, partic-

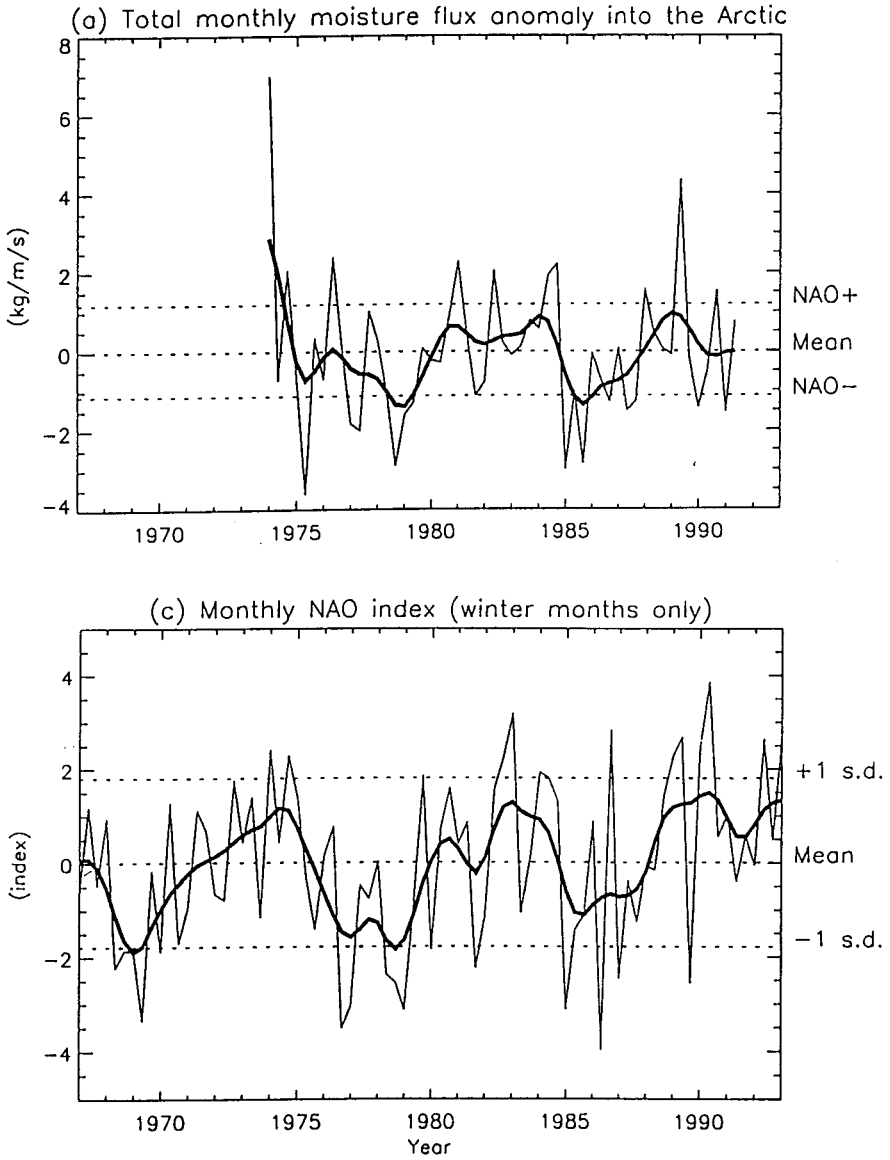

FIG. 6. (a), (b) Total winter moisture flux (kg m^{-1} s^{-1}) passing 70°N, 1974–91, for composites of NAO+ and NAO− winter months (DJF) compared with the winter (DJF) NAO index.

ularly in the boundary currents along the Siberian continental slope and up into the Canada Basin, the signal is undoubtedly real. This they attribute to an increased northward transport through the Fram Strait and the Barents Sea in the early 1990s, some warming of the inflow, and a reduced heat loss from the Atlantic layer in the Arctic Ocean as a result of a lesser formation of new ice on the Arctic shelves and thus a reduced warm water entrainment by brine plumes descending the Arctic Slope. The last-named effect is of relatively minor importance (discussed below, section 2e). Time dependence in the Atlantic water inflow and its temperature is identified as the primary cause of the observed warming, and it is here that the effect of the NAO and its changes is most evident.

After the split of the Norwegian Atlantic Current off northern Norway, Atlantic water enters the Arctic Ocean along two main pathways (Fig. 8). Grotefendt et al. (1998) and this report provide complementary descriptions of decadal hydrographic change and NAO relations along both of these branches. From his wind-driven barotropic model (Adlandsvik 1989; Adlandsvik and Loeng 1991; ICES 1996; Loeng et al. 1997), Adlandsvik suggests that the transport through the Barents Sea pathway increased by about a quarter since 1970. In Fig. 9, updated and adapted from Grotefendt et al. (1998), this transport time series (through line ''F'' in Fig. 8) is compared with the 0–200 m temperature change on the Kola section of the eastern Barents Sea (''K'' in Fig. 8; see Bochkov 1982; Adlandsvik and Loeng 1991;

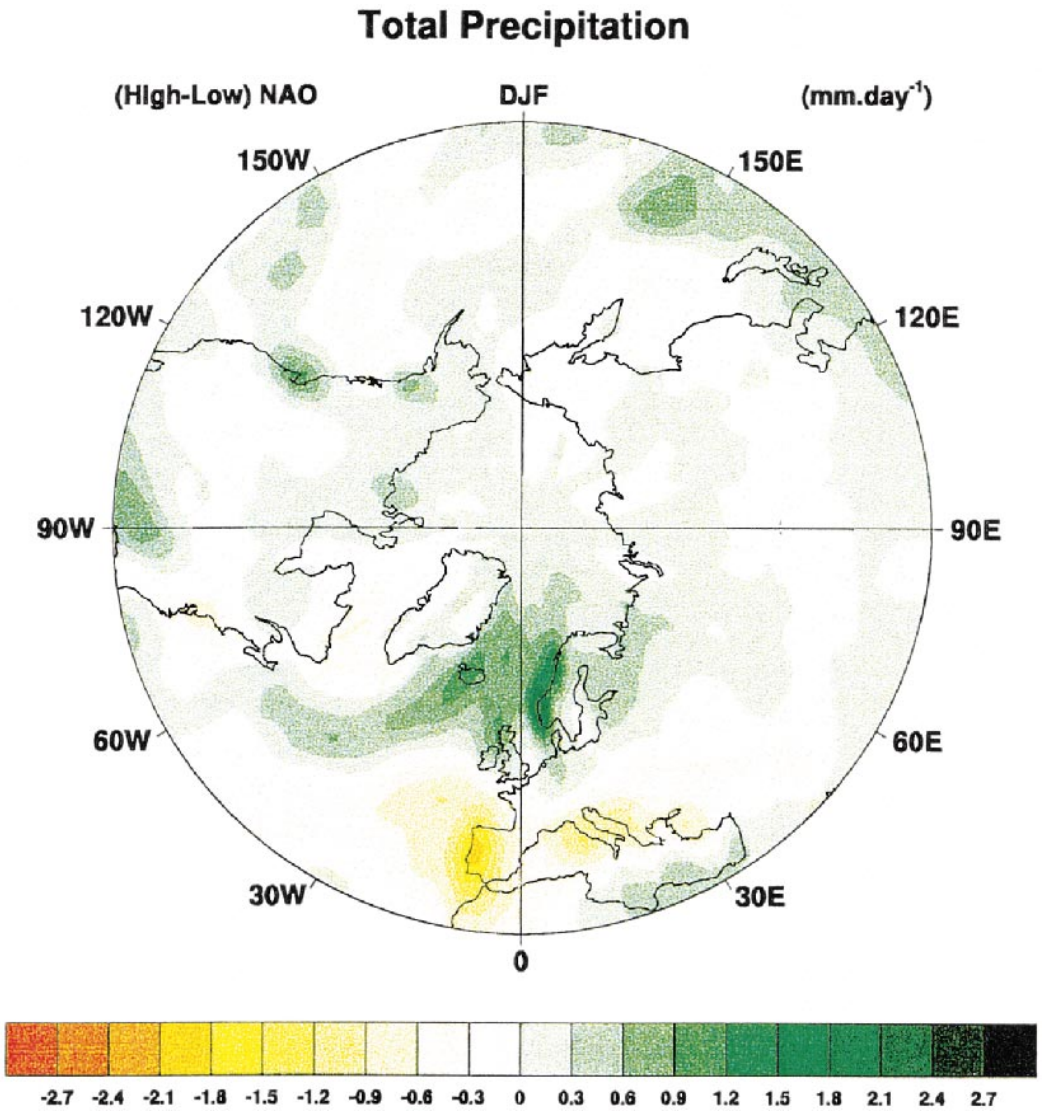

FIG. 7. Change in hemispheric winter precipitation between low-index NAO and high-index NAO composites of winter months [reconfigured from Xie and Arkin (1996)].

Bochkov and Troyanovsky 1996; Tereshchenko 1996) and with the winter NAO index of Hurrell (1995a). Plainly, there is a close correlation between all three variables. Very approximately, a 1-sigma change in the NAO index is associated with a 0.13 Sv change in inflow, and a 0.23°C temperature change in the east-central Barents Sea.

For the alternate warmer and more saline branch of the Atlantic current, which enters the Arctic Ocean through Fram Strait, we have no direct long-term current measurements or any equivalent model of warm water flux. Even the mean transport is uncertain. Grotefendt et al. (1998) suggest that of 3 Sverdrups (Sv $\equiv 10^6$ m^3 s^{-1}), which enter eastern Fram Strait from the south, 1 Sv of Atlantic water enters the Arctic and 2 Sv recirculate back to the Norwegian Sea, but admit that this is a short-term estimate, without any real point-of-reference to seasonal or longer-term fluctuations.

We have better information on hydrographic changes within the Atlantic water layer. Dickson and Blindheim (1984) used data from the annual O-Group fish surveys to construct time series of temperature, salinity, and σt for the zonal Sorkapp section along 76°20′N (''S'' in Fig. 8) from 1965–82, and Dickson et al. (1999) provide updates of these plots for two key stations at 9°E and 11°E, which monitor conditions in the Atlantic water core of the West Spitsbergen Current. Over almost the full period of the decadal change from low- to high-index NAO activity, these plots confirm that—as for the Barents Sea shelf—the long-term changes in the Fram Strait inflow are correlated with, and we suppose are driven by, the NAO. Regarding temperature, Fig. 10

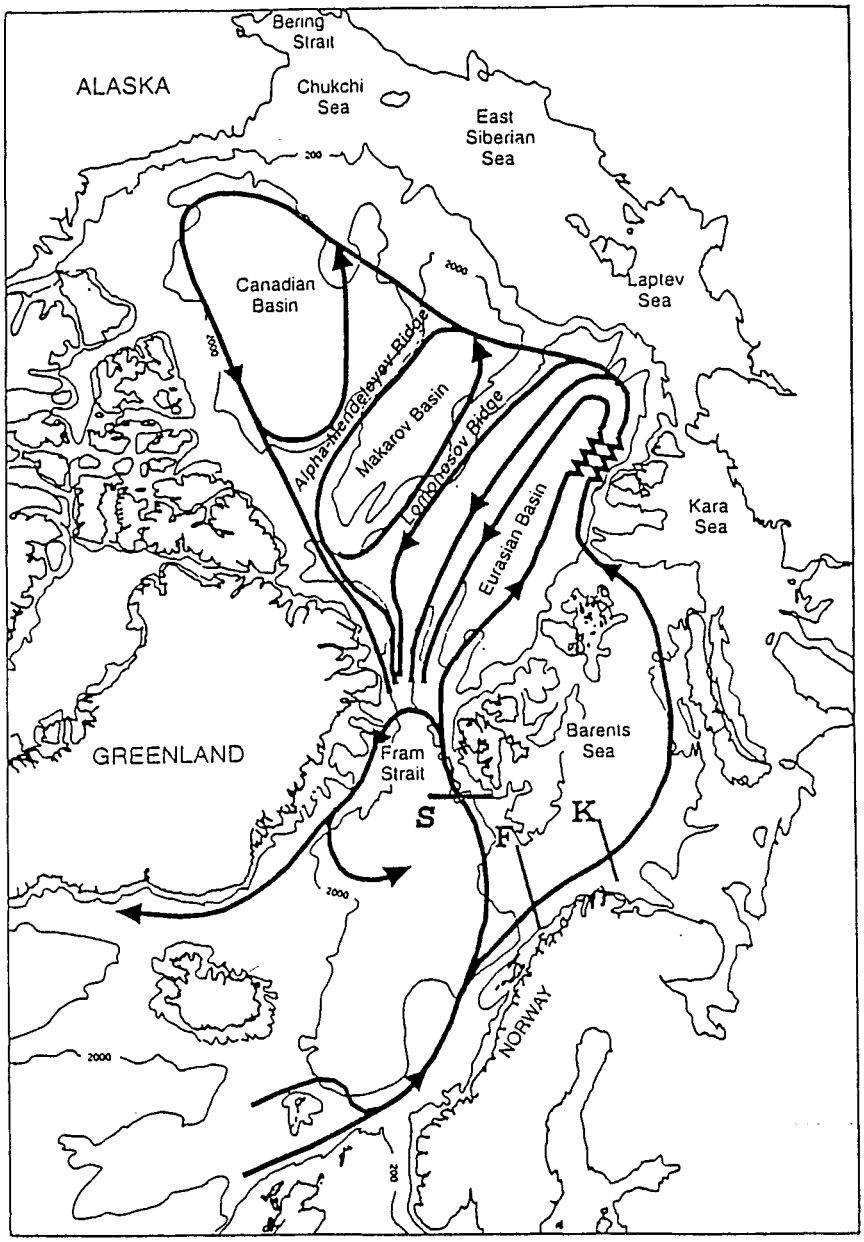

FIG. 8. The circulation of the Atlantic water layer in the Arctic Ocean and subarctic seas. Adapted from Grotefendt et al. (1998).

shows that the 50–500-m mean temperature at 9°E and 11°E on this section rose by approximately, 1°–2°C from the mid-1960s to the mid-1990s, with short-term peaks of about the same amplitude superimposed on this trend in the early 1970s, early 1980s, and early 1990s, thus reflecting both the long-term trend and interannual fluctuations of the NAO (lower panel, Fig. 10). The time series from discrete standard depths between 50 and 500 m (not shown) provide some indication that the warming trend is maximal in the upper 400 m, with a reduced amplitude at 500 m. Salinities show the opposite long-term trend (Fig. 11a), with means in the 50–500-m layer falling by between 0.033 and 0.050 over the period of record, so that mean densities decrease also, by about 0.1–0.15 kg m^{-3} (Fig. 11b). A similar freshening tendency affected the 50–200-m layer of the Barents Sea throughflow.

Swift et al. (1997) link these changes to events in the Arctic Ocean proper, showing that once the intervening distances and flow rates are taken into account, the anomaly and tendency of Atlantic-layer temperatures at various points around the Arctic Slope can be matched to interannual temperature changes on the Sorkapp section. The boundary current from Fram Strait is thus

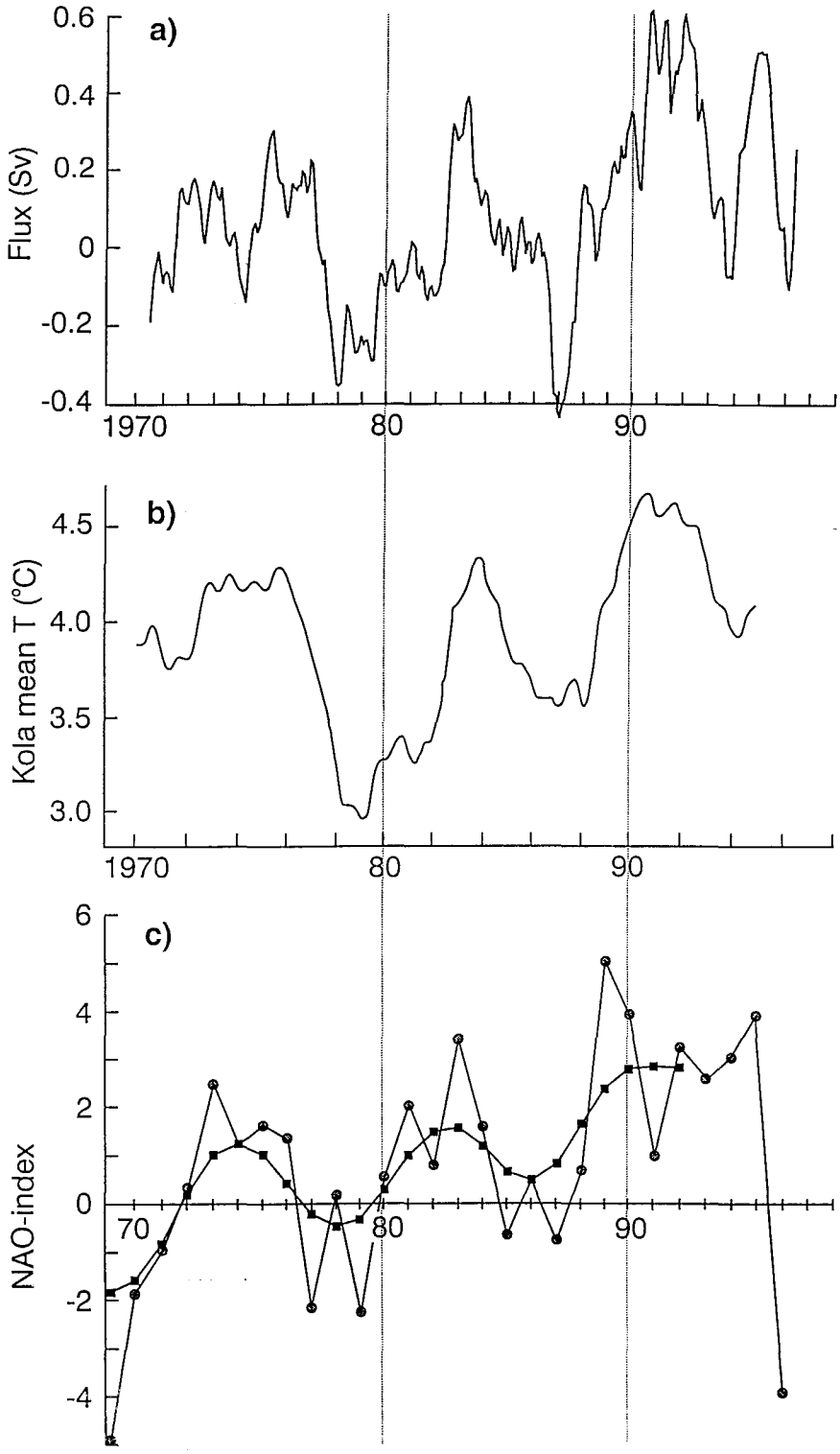

FIG. 9. (a) Moving 1-yr average of the atmospherically driven volume flux through the Fugloya–Bjornoya section of the western Barents Sea 1970–97 (Loeng et al. 1997, updated). (b) Monthly 0–200 m temperature anomalies from the Kola section of the east-central Barents Sea, 1970–95 (after Adlandsvik and Loeng 1991; Tereschenko 1996). (c) Winter (DJFM) NAO index (Hurrell 1995a). Adapted and updated from Grotefendt et al. 1998.

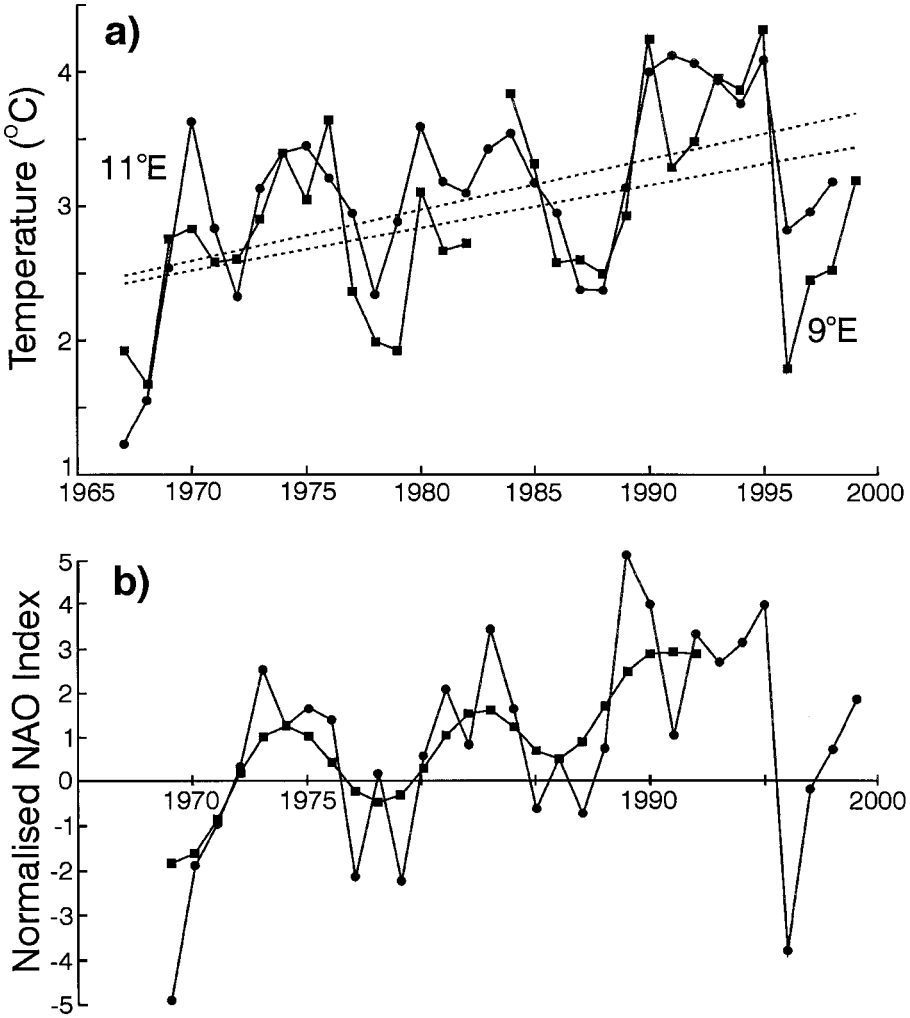

FIG. 10. Mean 50–500-m temperature (°C) in Aug–Sep at 9° and 11°E on the Sorkapp section, 1967–99, compared with the normalized winter NAO index (Hurrell 1995a).

demonstrated to be the main conveyor of the warming signal to the Arctic. Offslope spreading of the $\theta - S$ characteristics from the boundary current to the interior then takes place by intrusive layering (Carmack et al. 1997). As in the present report, Swift et al. suggest the NAO to be the ultimate cause of these changes in the character of the inflow, and were indeed the first to do so.

d. Sea level

Though direct measurements of the West Spitsbergen Current are too short to describe the time dependence of Atlantic inflow via this important branch, multidecadal sea level records have been suggested as a possible proxy. In a series of studies, Mandel (1976, 1978, 1979) uses the Barentsburg, Spitsbergen sea level record and local hydrography to provide estimates of the 0–500-m monthly and annual flux of Atlantic water and heat through the standard Barentsburg–Ice Edge Section between 1949 and 1978. He finds a long-term diminution in both to a minimum in the mid- to late 1960s (the time of the NAO minimum), consistent with our conclusion that the NAO *maximum* of the early 1990s was accompanied by record warmth along both inflow branches and increased inflow to the Barents Sea shelf (section 2c, above). He derives a linear relationship between Barentsburg sea level and Atlantic water inflow in the 0–500-m layer, such that

$$Q = 0.59h - 51.9,$$

where Q is the inflow in km^3 h^{-1} and h is the monthly or annual sea level (cm) at Barentsburg.

However, although Fig. 12 shows a clear correspondence between the changing winter sea level at Barentsburg and the winter NAO index since 1965, the connecting mechanism is unclear. In these waters, an increasingly positive NAO index represents both a de-

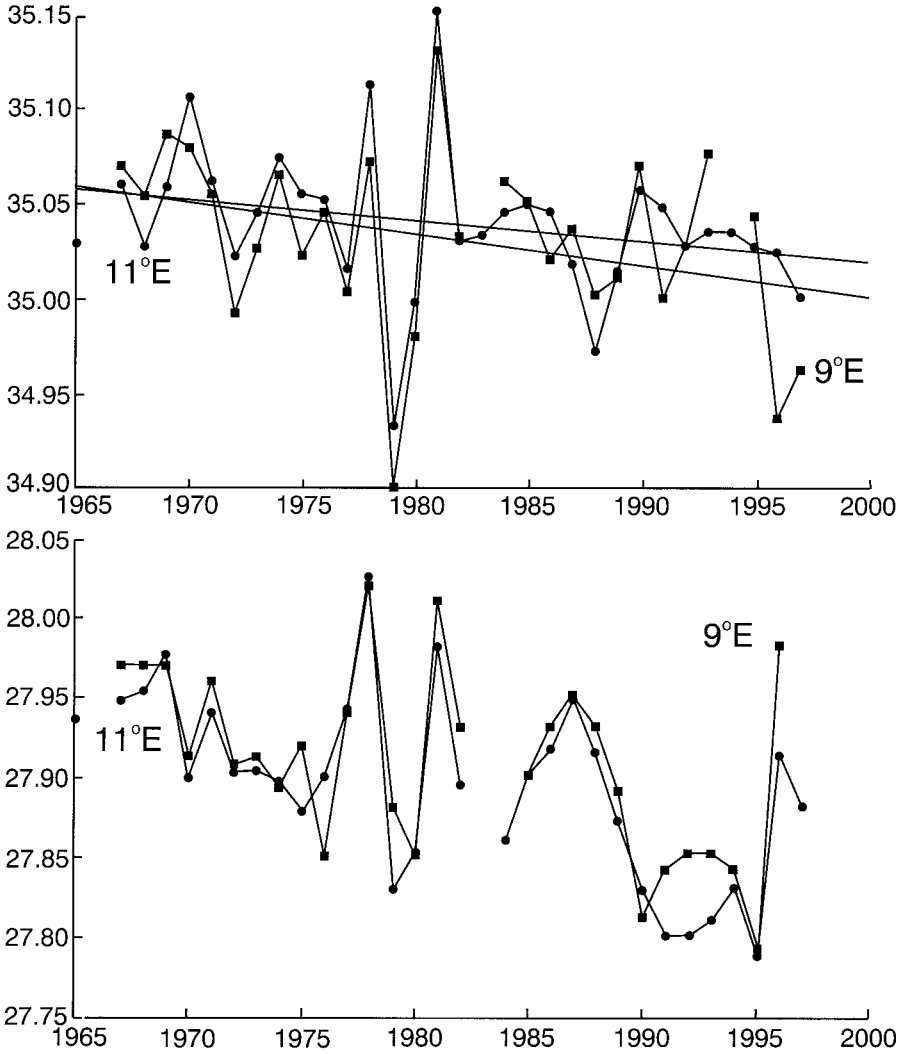

FIG. 11. Variation of 50–500-m mean salinity and density (σt) in Aug–Sep at 9° and 11°E on the Sorkapp section, 1967–97.

crease in SLP *and* an increase in southerly airflow over the Norwegian Atlantic Current (e.g., Fig. 2), with the likelihood of both a static and a dynamic response in sea level. While the latter is expected to dominate, we cannot yet separate the two contributions, and so cannot assume that sea level is a proxy for inflow strength in this instance and at this location (bottom pressure gauges will shortly be deployed on the upper continental slope north of Svalbard to resolve this issue).

e. Ice extent

By careful merging of the Special Sensor Microwave Imager (SSMI) and Special Sensor Microwave Radiometer (SSMR) passive microwave datasets, Maslanik et al. (1996) and Bjorgo et al. (1997) describe a quasi-linear decrease in the sea-ice cover of the Arctic amounting to a loss of 4.5% in ice extent and 5.7% in ice area since 1978 (see also Serreze et al. 1995a; Johannessen et al. 1995). Cavalieri et al. (1997) estimate the decrease to be 2.9% decade^{-1} for the Arctic as a whole during 1979–96. Parkinson (1992) provides evidence of associated changes in the length of the sea-ice season.

Bjorgo et al. provide no temporal or regional breakdown of this change, but contrary to the earlier conclusion of Chapman and Walsh (1993), Maslanik et al. show that the bulk of the reduction was concentrated in the Siberian sector of the Arctic (East Siberian and Laptev Seas). They suggest that the open water in this sector is the result of increased cyclone activity over the Central Arctic in recent years (e.g., Figs. 4c and 4d), with more frequent invasions of warm air and associated enhanced melt, earlier breakup, and increased poleward ice advection by offshore winds (the relative importance of icemelt vs ice-motion is unclear). If so, as we concluded earlier (section 1e), it need have little directly

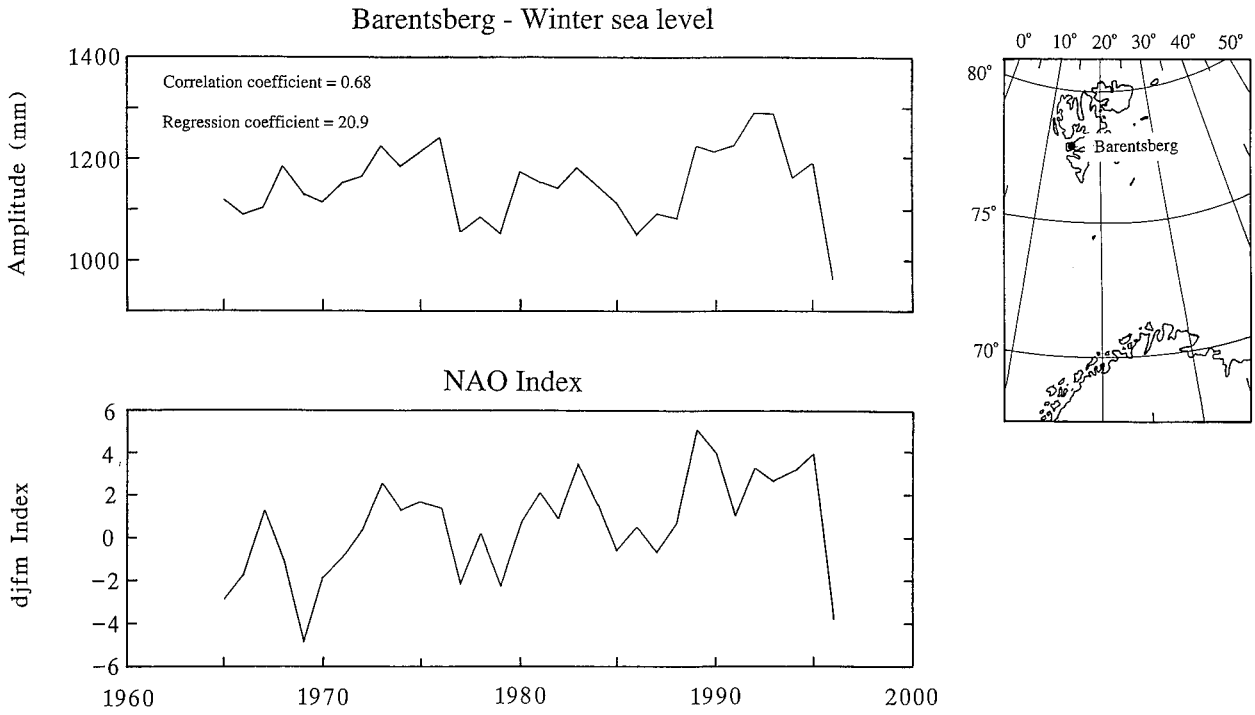

FIG. 12. Variation of winter mean sea level (mm) at Barentsberg compared with the winter NAO index, 1965–96.

to do with the North Atlantic oscillation, whose influence on the storm track seems to taper off rapidly toward the Arctic. Rogers and Mosley-Thompson (1995) would agree, arguing that recent mild winters over north-central Asia are not due to wind field changes associated with the NAO but to increased westerlies and cyclone warm sectors entering the region from other causes.

In keeping with the NAO focus of the present paper, we concentrate here on changes in the European Arctic and sub-Arctic sector where we *can* expect the anomalous wind field associated with extreme NAO activity to have a strong influence on sea-ice exent. For example, in his analysis of the Barents Sea ice margin over the past 400 yr, Vinje (1997) concludes that ''The extreme northern ice-edge positions in the sector in all probability coincide with an increased influx of water from the Norwegian Sea entering the Arctic Ocean north of Svalbard. . . .'' (see also Helland-Hansen and Nansen 1909). As just described, modeling work by Adlandsvik (1989) and Adlandsvik and Loeng (1991) had already demonstrated that variability in the Atlantic inflow is closely related to local wind conditions, while the recent studies by Grotefendt et al. (1998) have more specifically tied the Barents Sea influx to the NAO. A hypothetical chain linking the NAO with the ice edge is therefore already established for the Barents Sea and adjacent Arctic.

In the eastern parts of the European Arctic then, we can expect an extension of sea ice during the negative phase of the NAO, and sea-ice retraction during its positive phase, and this is what we observe. From ship, aircraft, satellite (after 1966), and other data, Fig. 13 describes the median ice border throughout both the western and eastern parts of the European Arctic at the time of the annual sea-ice maximum (April), compiled from the most extreme 7-yr runs of NAO− winters (1963–69) and NAO+ winters (1989–95), as identified in section 1b. Across this sector the change in the NAO between these extreme modes was accompanied by a reduction of 578 000 km^2 in ice extent. (Note that since there has been a general long-term retraction of sea ice in the Northeast Arctic over recent decades, some part of this change may be associated with hemispheric warming rather than the changing NAO; Vinje 1997.)

Important detail has been added recently by Deser et al. (2000), who use a 40-yr dataset (1958–97) to examine the association between wintertime sea-ice variability, air temperature, SLP, and the NAO in the European Arctic. They show a clear downward trend over this period in the leading EOF of winter sea-ice concentration anomalies, demonstrate that the large-scale SLP changes associated with this trend are reminiscent of the positive polarity of the NAO, and show a correlation of −0.63 between the principal component of ice concentration and the NAO index. They conclude therefore that *''the recent and historically unprecedented trends in the wintertime NAO and AO circulation patterns over the past three decades have been imprinted upon the distribution of Arctic sea ice.''* However, they also conclude that the changes in cyclone activity and SLP are not simply a reflection of the anomalous NAO circulation but may be a more direct response to

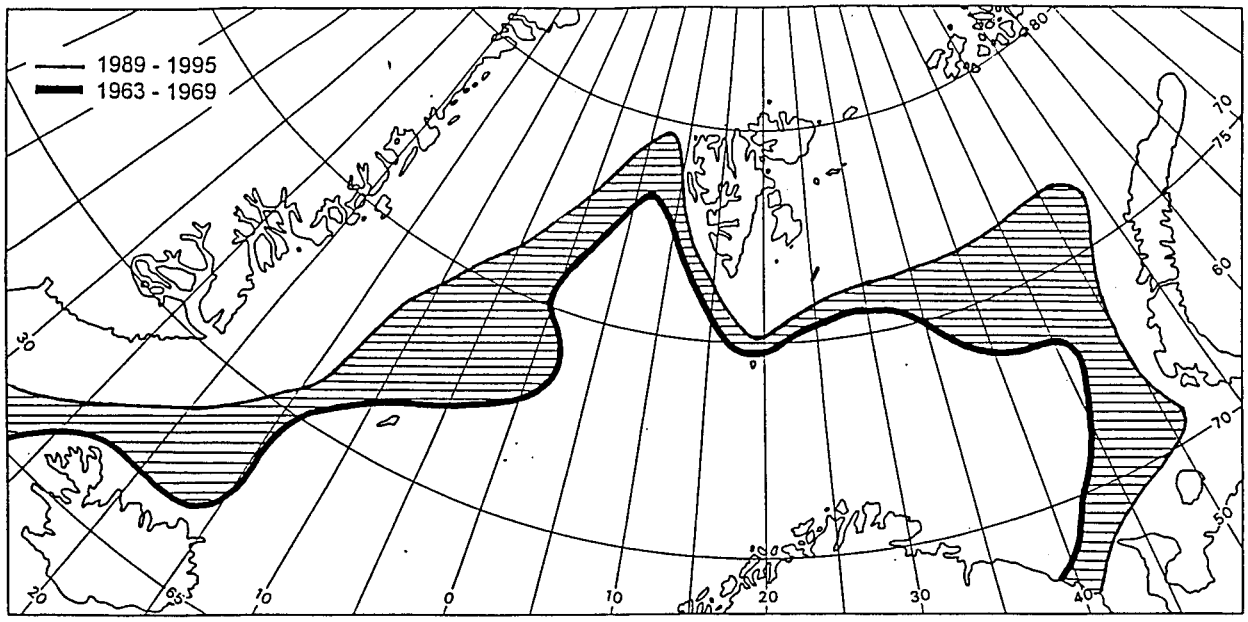

FIG. 13. The median ice border at the end of Apr for the periods 1963–69 and 1989–95, corresponding, respectively, to minimum and maximum phases of the NAO index. The more northern position of the ice edge for the period 1989–95 corresponds to a reduction in ice extent of about 587 000 km^2 from the period 1963–69.

the changes in sea ice itself, prompting the suggestion that an increasing sensible and latent heat flux directly over the reducing ice cover of the Greenland Sea may have contributed to the observed increase in the number of cyclones in that sector.

The effect of a change in ice cover on the input of heat to the Arctic is also one of the factors assessed by Grotefendt et al. (1998). Providing that the reduced ice extent in the Barents Sea during the 1990s was due to diminished winter ice production rather than increased summer meltback, it should result in a lesser drainage of brine down the Arctic Slope, and a reduced warm-water entrainment by the sinking plumes. Because the reduction in Fig. 13 is measured at the end of winter, it would seem to indicate the former cause (i.e., decreased production). Even so, Grotefendt et al. calculate that the Atlantic Layer would experience a warming of only 0.15°C from this effect, much less than the observed ''Arctic Warming'' signal.

f. Summary: Inputs

We would conclude with Swift et al. (1997) and Grotefendt et al. (1998) that the so-called Arctic warming is partly or primarily the result of multidecadal variability in the NAO and arises largely outside the Arctic Ocean. As the winter NAO index increased from its lowest values of record (generally) in the 1960s to its highest-ever values during the early 1990s (see Fig 1), the increasingly anomalous southerly airflow that accompanies such a change over the Nordic Seas (cf. Figs. 2c and 2d) is held responsible for a progressive warming in the two streams of Atlantic water that enter the Arctic Ocean across the Barents Sea shelf and along the Arctic Slope west of Spitsbergen. By the late 1980s–early 1990s, when the NAO reached an interannual and interdecadal maximum, the superposition of a short-term warming event on the long-term warming trend meant that both Atlantic-inflow streams were running between 1° and 2°C warmer than normal. Adlandsvik's barotropic model suggests that the transport through the Barents Sea pathway may have increased by about a quarter at this time, as Grotefendt et al. point out, and we have possible proxy evidence from sea level records to suggest that the West Spitsbergen Current was similarly boosted. From the Sorkapp section, we have evidence that the warming of the inflow through Fram Strait was accompanied by a progressive freshening tendency and a decreasing density in the upper 500 m since the 1960s, and the indications are that freshening also affected the Barents Sea branch of the Atlantic Current. Because the increasing NAO is associated with an increased summer meltback/decreased winter production of sea ice in the marginal ice zone of the Nordic seas, with (at least during the 1990s) an increased import of Arctic sea ice to the Greenland Sea through Fram Strait (section 3a below) and with a major increase in precipitation along the length of the Norwegian Atlantic Current ($\Delta P \approx +15$ cm per winter for NAO+ minus NAO− conditions; Fig. 7), a broadscale freshening throughout the Atlantic water domain is not unexpected. An increasing heat flux from a decreasing sea-ice cover may have locally helped to stimulate an already high winter cyclone frequency in this sector.

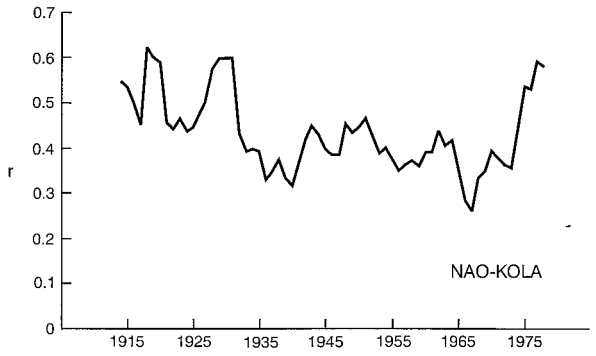

FIG. 14. The 30-yr moving correlation between the winter NAO index and the annual 0–200-m temperature on the Kola section of the Barents Sea, plotted against the center year of each period.

Thus the Arctic warming of the early 1990s appears to be the combined result of a warmer and probably stronger inflow of Atlantic water along both of the main inflow branches as the NAO index built to its most prolongued and extreme positive values of record. The major retraction in winter sea-ice extent that accompanied this change may have helped to preserve the warmth of the Atlantic inflow to the Arctic where it passes as a boundary current along the Eurasian Slope if it acted to reduce brine drainage and warm water entrainment, but this effect is regarded as minor.

Though the link between the NAO index and inflow temperature appears strong for both inflow branches (Figs. 9 and 10), we are aware of other strong correlations involving the NAO that have proved to be time dependent. For example, the well-established and close correlation between the winter NAO and the seesaw in winter temperatures between Greenland and Europe broke down abruptly but temporarily in the 1920s and 1930s (see Rogers 1994, his Fig. 2). We therefore checked the robustness of the relationship between the winter NAO and monthly 0–200 m Kola mean temperatures by constructing 30-yr moving correlations between the two variables over the whole of this century. The results are plotted against the central year of each 30-yr period in Fig. 14. As shown, though the relationship does not break down, it is markedly stronger during the early years of the century and recently (corresponding roughly to the positive phases of the NAO, when the storm track penetrates to the Barents Sea) than in the intervening decades (see ICES 1996).

Although a warming of both inflows might be thought to have implications for the mass balance of sea ice in the Eurasian Basin, concern is probably more appropriately focused on the recent retreat of the cold halocline layer (CHL), which insulates the Arctic Ocean surface and sea ice from direct contact with the warm Atlantic layer below. Steele and Boyd (1998) document a retraction of the CHL from the Amundsen to the Makarov Basin during the 1990s, and hydrography, tracers, and modeling all suggest that this change stemmed from the eastward diversion of Russian river input in response to the altered atmospheric circulation.

3. Adjustments and outputs

a. Fram Strait ice flux

Close to 90% of the ice that leaves the Arctic Ocean through the Fram Strait passes south through 0°–10°W (Vinje et al. 1998), making this a key site for estimating its net production. For some years now, estimates of the ice area flux have been possible using drift speeds derived from satellite imagery or buoy drifts, and stream widths measured from ice maps (e.g., Zakharov 1976; WMO 1994). The establishment of a relationship between ice draft and ice thickness for Fram Strait by ice drilling in the early 1980s, and continuous measurements of ice draft using moored upward looking sonars have together permitted the accurate monitoring of ice thickness since 1990 (Vinje et al. 1998). The resulting volume-flux series shows a significant interannual variation from a minimum of 2046 $km^3\ yr^{-1}$ in 1990–91 to 4687 $km^3\ yr^{-1}$ in 1994–95, and since annual mean ice thickness does not alter by more than $\pm 10\%$, and has not for the last 2–3 decades (Vinje et al. 1998, their Table 4), this variability is largely ascribed to changes in area flux due to changes in the wind field. [''Over 80% of the variance in daily ice drift in the central Arctic is explained by winds'' (Serreze et al. 1992, p. 293)]. A maximum in the area flux in 1994–95 seems to confirm that assumption, and the general interannual maximum in area flux in 1990–96 compared with earlier estimates is tentatively ascribed by Vinje et al. to the increased cyclonic circulation in recent years, described by Walsh et al. (1996; see Fig. 4c).

However interannual and longer-term changes in the NAO, which have been extreme in recent years, can equally influence the Arctic pressure field (Fig. 2) and may affect the ocean circulation also through effects on the freshwater flux and on the temperature and salinity of its Atlantic water inputs (sections 2a–c above).

Against the recent changes in the winter NAO index (dashed line), Fig. 15 describes the variability in the volume flux of ice through Fram Strait based on a range of estimates and assumptions, but constrained by the accurate measurements of Vinje et al. for the years since 1990. For the full period since 1976, the time series of Vinje and Finnekasa (1986) have been adjusted to the measurements of Vinje et al. (1998) by Alekseev et al. (1997), using the relationship between these recent data and the cross-Strait atmospheric pressure gradient between Nord, Greenland, and Barentsburg, Spitsbergen. The choice of pressure gradient is a matter of debate and could certainly be optimized. Vinje et al. [1998, their Eq. (4)] suggest that the pressure gradient between 81°N, 10°W and 73°N, 20°E may be a better determinant of the transpolar ice drift, because it explains 89% of the variance in the measured ice velocity in Fram Strait,

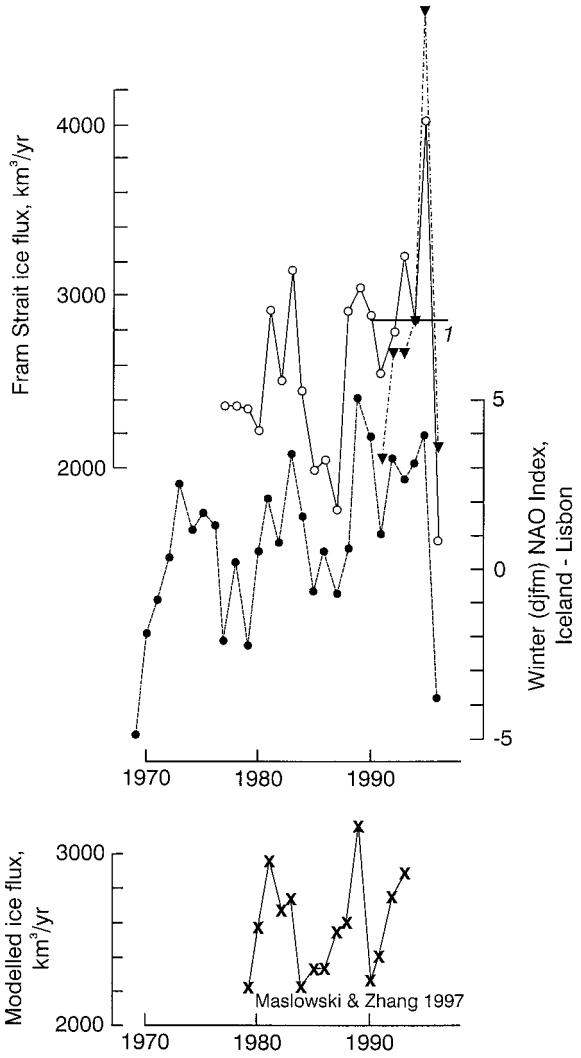

FIG. 15. Comparison of the winter NAO index with the observed, estimated, and modeled Fram Strait volume flux of ice since 1976. ○– – –○ Volume flux series merging the estimates of Vinje and Finnekasa (1986) and Vinje et al. (1998) (Alekseev et al. 1997). ▼– – –▼ Estimates based on direct measurements, 1990–96 by Vinje et al. (1998). ●– – –● The winter (DJFM) NAO index (from Hurrell 1995a). ×– – –× Modeled ice flux using the ECMWF reanalysis, 1979–93 (W. Maslowski and Y. Zhang 1998, personal communication). 1 = mean of the measured/estimated flux (Vinje et al. 1998).

and this version of the ice flux calculation is also shown in the upper panel of Fig. 15. As shown, the winter NAO index explains about 63% of the variance in the annual efflux of ice since 1976 (Fig. 17b) so that, very approximately, a 1-sigma change in the winter NAO index is associated with a 200 km^3 change in annual ice flux.

We have a variety of ways of checking whether our recent estimates of the relative interannual changes in the efflux of ice from Fram Strait are likely to be sound. A very similar time dependence of the area flux of ice has recently been derived for an 18-yr period by Kwok and Rothrock (1999) through tracking the displacement of common sea-ice features in sequential 85 GHz and 37 GHz brightness temperature fields during winter (October–May). These authors also emphasize the strong positive relationship with the NAO index. Modern simulations provide further confirmatory evidence. The mean simulated volume flux by Harder et al. (1998; 2870 km^3 yr^{-1}) compares well with the mean of measurements from 1990–96 by Vinje et al. (1998; 2843 km^3 yr^{-1}; bar ''1'' in Fig. 15). Figure 15 also describes output from the Advanced Arctic Ocean Model with Sea-Ice recently developed at Navy Postgraduate School, Monterey (W. Malowski 1998, personal communication; Zhang et al. 1999). A 15-yr integration of this high-resolution 30-layer model, driven by a new ECMWF reanalysis for 1979–93, shows annual averages of the Fram Strait ice flux, which vary from 2200 to 3150 km^3 yr^{-1}, with a mean of 2555 km^3 yr^{-1}. Clearly, both the scaling and the time dependence of the simulated volume flux are well matched to the observed flux and its supposed forcing over this 15-yr period, suggesting that the essential dynamics of ice transport through Fram Strait are adequately captured by the model.

Because there is no very obvious time lag between forcing and flux, these observed and simulated series also appear to confirm the dominance of direct regional wind forcing over broadscale changes in the Arctic Ocean circulation in determining the year-to-year variability of ice flux. The dominant wind forcing in recent years has been the anomalous airflow associated with the extreme positive phase of the NAO.

b. The GSA paradox

Over the past two decades, then, which include our best and most complete datasets, there seems unanimity that the ice flux and positive NAO are closely linked. The question is whether this (or indeed *any*) link with the NAO is robust in the longer term. In the 40-yr simulated ice flux series, which Harder et al. (1998) derive from their dynamic/thermodynamic sea-ice model, forced by NCEP–NCAR (reanalysis) winds and temperatures, they find a close fit between ice flux and NAO over the past two decades but very little correspondence in earlier years (Harder et al. 1998, their Fig. 2c). Similarly, the correlation that Kwok and Rothrock (1999) derive between the NAO index and their satellite-based series of ice flux estimates is good during the years of the positive NAO but degrades during earlier (NAO−) years. In a 50-yr series of ice flux estimates recently derived by T. Vinje (1999, personal communication), any simple correlation that now exists with the NAO breaks down so that increased efflux can occur in both the high- and low-index phases of the NAO. The case of the Great Salinity Anomaly (GSA; Dickson et al. 1988) provides some insight as to why.

The term GSA describes the anomalous increase by

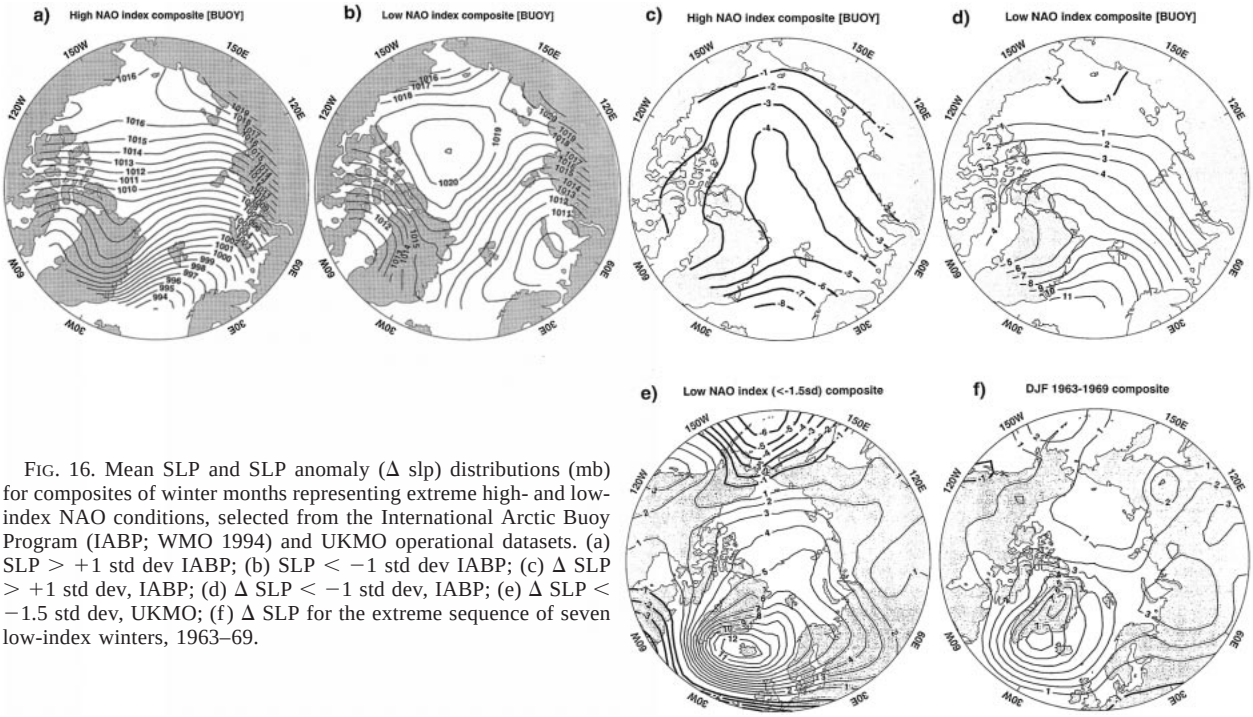

FIG. 16. Mean SLP and SLP anomaly (Δ slp) distributions (mb) for composites of winter months representing extreme high- and low-index NAO conditions, selected from the International Arctic Buoy Program (IABP; WMO 1994) and UKMO operational datasets. (a) SLP $> +1$ std dev IABP; (b) SLP < -1 std dev IABP; (c) Δ SLP $> +1$ std dev, IABP; (d) Δ SLP < -1 std dev, IABP; (e) Δ SLP < -1.5 std dev, UKMO; (f) Δ SLP for the extreme sequence of seven low-index winters, 1963–69.

some 2000 km^3 in the southward transport of ice and freshwater by the East Greenland Current during the 1960s (Aagaard and Carmack 1989), preserved through the cessation of winter convection north of Iceland, passing out to the open Atlantic through Denmark Strait in the late 1960s, and traceable thereafter around the subpolar gyre for over 14 yr until its return to the Greenland Sea in 1981–82 (Dickson et al. 1988). As Aagaard and Carmack point out, such an anomaly could be explained only by a major increase in the outflow of ice and freshwater from Fram Strait, but if so, it occurred at a time when the NAO index was at its most protracted and extreme *negative* state of record (Fig. 1).

This paradoxical association of the Fram Strait ice flux *both* with extreme positive *and* negative states of the NAO is explained in Figs. 16a–f. Composites of absolute and anomalous SLP for winter months >1 std dev from the NAO mean and based on the most highly resolved dataset (that of the Arctic drifting buoy program; Figs. 16a,b and 16c,d) describe a strengthened northeasterly airflow in the approaches to Fram Strait during high-index conditions, which should assist the southward efflux of ice, while that during low-index conditions (e.g., Fig. 16d) should oppose it. Switching to the UKMO operational dataset in order to have access to the lowest-index winters of the 1960s (the International Arctic Buoy Program began in 1979), a composite of low-index months >1.5 std dev from the NAO mean shows that an anomalous southwesterly airflow still prevails there in these more extreme conditions. (Fig. 16e). Only when the SLP composite is formed from the specific 7-yr sequence of extreme low-index winters that prevailed during the 1960s (1963–69; Fig. 16e) does a seemingly minor change in the alignment of the pressure field direct a northwesterly anomalous airflow over Fram Strait.

We conclude from this that the NAO index is *not* simply correlated with ice flux through Fram Strait, that conditions conducive to ice flux can occur during both extrema of the NAO, that the closest correspondence between increased ice flux and the NAO occurs during NAO+ conditions, but that (if the conditions of the GSA case can be considered as representative!) an enhanced efflux can occur during the opposite extreme state of the NAO. Because the latter would occur at a time when the ice flux is generally reduced, this ''event'' may appear more conspicuous by contrast, as with the GSA.

4. Summary

This study has aimed to synthesise results from existing studies and rework a broad range of other datasets to identify the Arctic–sub-Arctic response to the NAO in the broadest possible range of parameters. The following appear to be the key elements of that response.

1) The North Atlantic oscillation (NAO) is the dominant recurrent mode of atmospheric behavior across the Arctic Ocean. The North Pacific (NP) pattern becomes dominant, on average, only south of the Bering Strait. Between low-index and high-index extreme states of the NAO, mean winter SLPs

decrease throughout the Arctic and sub-Arctic from a center of maximum change over Iceland and the Iceland Sea (−22 hPa in the UKMO dataset used here) to a line of zero change near the Bering Strait.

2) The NAO index exhibits a considerable decadal variability that appears to be amplifying with time. Thus in a record extending back to 1865, the NAO index evolved to its most persistent and extreme negative state in the 1960s, and thereafter to an equally extreme positive state in the late 1980s–early 1990s (Hurrell 1995a, updated).
3) This gradual evolution from low- to high-index conditions in winter brought the expected northeastward extension of the Atlantic storm track to the Greenland, Iceland, Norwegian, and Barents Seas (Serreze et al. 1997; Alexandersson et al. 1998) together with an increase in the numbers of deep Atlantic storms from near-zero during low-index conditions to around 15 per winter during the high-index phase. An increasing heat flux from a decreasing sea-ice cover may have locally helped to stimulate an already high winter cyclone frequency in the Nordic Seas (Deser et al. 2000). However, a sharp increase in cyclone frequency north of 75°N and decreased SLP over the central Arctic from the late 1980s are not obviously or simply the effects of the NAO (Maslanik et al. 1996; Walsh et al. 1996).
4) These decadal shifts in the winter NAO and storm track are associated with major changes in the freshwater supply to high latitudes, especially in the European Arctic and subarctic. Modern datasets on moisture flux (Serreze et al. 1995c) and precipitation (Xie and Arkin 1996) are available only from 1974 and l979, respectively, so that low-index extrema are underrepresented. Nevertheless, between composites of winter months representing low-index and high-index conditions, the total net moisture flux through 70°N increases from 4.4 to 7.6 $\times$ 10^7 kg s^{-1}, and the proportion that passes north through the Nordic Seas–Scandinavia sector (10°W to 50°E) increases from 0% to 58%. The major precipitation change also takes place in this sector, increasing by about 15 cm per winter along the length of the Norwegian Atlantic Current between low-index and high-index extrema. Though we cannot yet assign a cause to this change in the precipitation balance of the sub-Arctic, similar changes, with global effects, appear to be anticipated in the recent results of coupled climate models (Manabe and Stouffer 1993, 1994; Rahmstorf and Ganopolski 1999).
5) The ''Arctic warming'' observed in the Atlantic-derived sublayer of the Eurasian Basin during the early-to-mid 1990s is larger than can be explained by noise in the data (Grotefendt et al. 1998) and is attributed largely to the same multidecadal evolution in the NAO index. Specifically, direct and proxy evidence suggests that the warming is the combined result of a warmer and stronger inflow of Atlantic water along both the main inflow branches as the NAO index built to its most prolonged and extreme positive values of record. There is no obvious lag between NAO index and inflow temperature. At the peak, both Atlantic inflow streams were observed to be running between 1° and 2°C warmer than normal. Modeling suggests that the barotropic component of Barents Sea inflow increased by about 25%, and the Barentsburg (Spitsbergen) winter sea level rose to its highest postwar values, with the (still tentative) suggestion that the more important (warmer, saltier) west Spitsbergen branch was also boosted under these conditions. Very approximately, a 1-sigma change in the NAO index is associated with a 0.13 Sv change in the Barents Sea throughflow, a 0.23°C temperature change in 0–200 m monthly mean temperature along the Kola section of the east-central Barents Sea, and a 0.35°C mean change in the 50–500-m layer of the West Spitsbergen Current in late summer.
6) Salinities along both inflow branches appear to have declined as the NAO evolved from its low-index extreme of the 1960s to its high-index extreme of the 1990s, consistent with the increasing freshwater accession, increasing volume flux of ice from the Arctic (Vinje et al. 1998) and reduction in sea ice over this period (Deser et al. 2000). In the 50–500-m layer of the Sorkapp section, the decrease in mean salinity was between 0.033 and 0.050, resulting in a decrease in the mean density of this layer by 0.1–0.15 kg m^{-3}.
7) The increased flux of heat to the Barents Sea and adjacent Arctic was accompanied by a marked retraction of sea ice, part of a general reduction of 578 000 km^2 in the median ice extent across both the western and eastern parts of the European Arctic between the low-index (winters 1963–69) and high-index (winters 1989–95) extrema of the NAO. During 1958–97, the time dependence of winter sea-ice concentration around the Nordic Seas is significantly and negatively correlated with the NAO index (Deser et al. 2000). Providing the reduced ice extent in the Barents Sea during the 90s was due to diminished ice production in winter rather than increased summer meltback, it should result in a lesser drainage of brine down the Arctic Slope, and a reduced warm-water entrainment by the sinking plumes (Grotefendt et al. 1998). However, this contribution to ''Arctic warming'' is expected to be minor.
8) The interannual variations of the winter NAO index explain about 60% of the variance in the annual volume flux of ice through Fram Strait since 1976; a 1-sigma change in the winter NAO index is then associated with a $\approx$200 km^3 change in annual ice

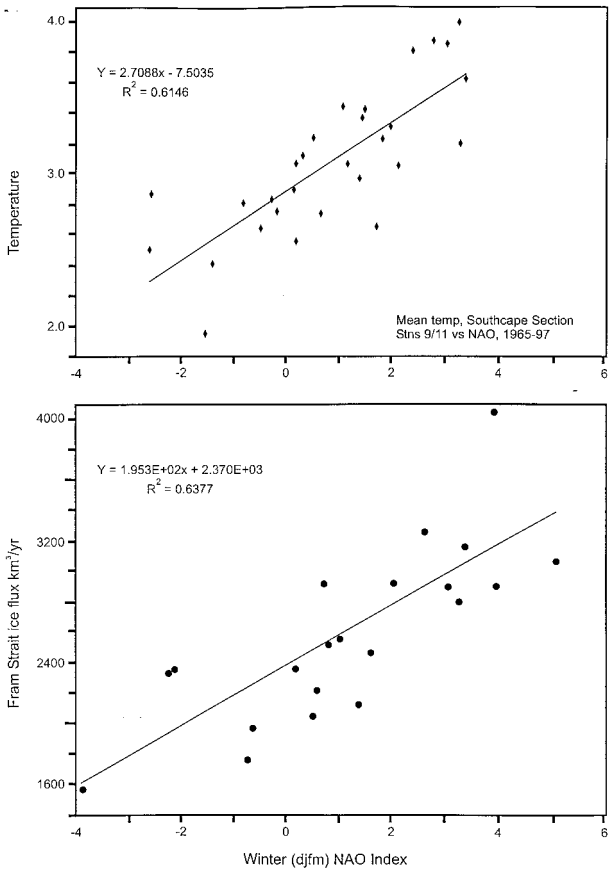

FIG. 17. Correlations between the winter NAO index and (a) the mean 50–500-m temperature (°C) at stations 9° and 11°E on the zonal Sorkapp section along 76°20′N, southwest of Spitzbergen (''S'' in Fig. 8) from 1965 to 1997, and (b) the annual volume flux of ice through western Fram Strait since 1976, (km^3 yr^{-1}). Because the Sorkapp temperatures are inherently noisy, being based on a single CTD cast per year at each station, the series in (a) have been smoothed with a 3-yr running mean before correlating.

flux. A recent 15-yr integration of the Naval Postgraduate School Advanced Arctic Ocean Model with Sea Ice, driven by the new ECMWF reanalysis for 1979–93, shows a simulated volume flux that is well matched to the observed flux and its supposed forcing. Because there is no very obvious time-lag between forcing and flux, these observed and simulated series appear to confirm the dominance of direct regional wind forcing over broad-scale changes in the Arctic Ocean circulation in determining the year-to-year variability of ice flux.

9) Although the Fram Strait ice flux shows a strong correspondence with the positive phase of the winter NAO index, the ice flux is not strictly correlated with the NAO. The case of the Great Salinity Anomaly (GSA) of the 1960s demonstrates that large anomalies in the flux of ice and freshwater are not unknown during the extreme opposite (low index) phase of the NAO index. The latter are likely to be eventlike and conspicuous but may be of comparable magnitude to the ice flux maxima observed during the 1990s. The estimated 2000 km^3 of extra ice and freshwater brought south by the GSA in the mid-1960s (Aagaard and Carmack 1989) compares to a 1-yr increase of 1826 km^3 in the flux of ice alone observed in the Fram Strait between 1993–94 and 1994–95 (Vinje et al. 1998).

10) Regarding the two questions that partly motivated this study, we conclude that variations in the winter NAO index *currently* explain about 60% of the variance in the monthly depth-integrated temperature of the warmer, more saline (and therefore more important) Fram Strait branch of Atlantic water inflow to the Arctic Ocean since 1965 (Fig. 17a). Over the past 25 yr, the NAO also explains about 60% of the variance in the volume flux of ice through western Fram Strait (Fig. 17b). We suspect, however (Fig. 14 and section 3a), that neither relationship is robust in the longer term.

Acknowledgments. This paper could not have been put together without inputs of data and advice from many sources. We thank Mark Serreze of the University of Colorado and his coworkers for permission to use their dataset on moisture flux through 70°N (Fig. 5); Pingping Xie and colleagues at NCEP, for the use of their enhanced dataset on global precipitation; Tasos Kentarchos of the University of East Anglia for his help in working up the Arctic Ocean dynamic height data and moisture fluxes; Dr. Ian Vassie of Proudman Oceanographic Laboratory, Bidston, United Kingdom, for advice on Arctic sea level changes; Professor N. Smirnov and Professor V. Zakharov of AARI for their helpful provision of data, advice, and interpretation; and Dr. John Walsh of the University of Illinois for help and encouragement.

REFERENCES

Aagaard, K., and E. C. Carmack, 1989: The role of sea ice and other fresh water in the Arctic circulation. *J. Geophys. Res.,* **94,** 14 485–14 489.

——, and Coauthors, 1996: US, Canadian researchers explore Arctic Ocean. *Eos, Trans. Amer. Geophys. Union,* **77,** 209, 213.

Adlandsvik, B., 1989: Wind-driven variations in the Atlantic Inflow to the Barents Sea. ICES CM Mimeo 1989/C:18, 13 pp. [Available from ICES Secretariat, Palaegade 2–4, DK-1261, Copenhagen-K, Denmark.]

——, and H. Loeng, 1991: A study of the climate system in the Barents Sea. *Polar Res.,* **10,** 45–49.

Alekseev, G. V., O. I. Myakoshin, and N. P. Smirnov, 1997: Variability of sea ice transport through Fram Strait (in Russian). *Meteor. Hydrol.,* **N9,** 52–57.

Alexandersson, H., T. Schmith, K. Iden, and H. Tuomenvirta, 1998: Long-term variations of the storm climate over NW Europe. *Global Ocean Atmos. Syst.,* **6,** 97–120.

Bacon, S., and D. J. T. Carter, 1993: A connection between mean wave height and atmospheric pressure gradient in the North Atlantic. *Int. J. Climatol.,* **13,** 423–436.

Baldwin, M. P., X. Cheng, and T. J. Dunkerton, 1994: Observed correlations between winter-mean tropospheric and stratospheric circulation anomalies. *Geophys. Res. Lett.,* **21,** 1141–1144.

Bjorgo, E., O. M. Johannessen, and M. W. Miles, 1997: Analysis of merged SMMR–SSMI time-series of Arctic and Antarctic sea ice parameters 1978–1995. *Geophys. Res. Lett.,* **24,** 413–416.

Bochkov, Y., 1982: Historical data on water temperature in the 0–200m layer in the Kola section in the Barents Sea (1900–1981) (in Russian). *Ecology and Fisheries for Demersal Fish on the North-European Basin,* A. I. Mukhin, Ed., PINRO, 133 pp.

——, and F. M. Troyanovsky, 1996: Present day climatic variations in the Barents and Labrador Seas and their biological impact. NAFO Sci. Counc. Res. Doc. 96/25, 1–24. [Available from NAFO Secretariat, 2 Morris Drive, P.O. Box 638, Dartmouth, NS, Canada.]

Carmack, E. C., R. W. Macdonald, R. G. Perkin, F. A. McLaughlin, and R. Pearson, 1995: Evidence for warming of Atlantic water in the southern Canadian Basin of the Arctic Ocean: Results from the Larsen-93 Expedition. *Geophys. Res. Lett.,* **22,** 1061–1064.

——, and Coauthors, 1997: Changes in temperature and tracer distributions within the Arctic Ocean: Results from the 1994 Arctic Ocean section. *Deep-Sea Res. II,* **44,** 1487–1502.

Carter, D. J. T., 1999: Variability and trends in the wave climate of the North Atlantic: A review. *Proc. Ninth ISOPE Conf.,* Brest, France, International Society of Offshore and Polar Engineers, 12–18.

Cavalieri, D. J., P. Gloerson, C. L. Parkinson, J. C. Comiso, and H. J. Zwally, 1997: Observed hemispheric asymmetry in global sea ice changes. *Science,* **278,** 1104–1106.

Cayan, D. R., 1992a: Latent and sensible heat flux anomalies over the northern oceans: The connection to monthly atmospheric circulation. *J. Climate,* **5,** 354–369.

——, 1992b: Variability of latent and sensible heat fluxes estimated using bulk formulae. *Atmos.-Ocean,* **30,** 1–42.

——, 1992c: Latent and sensible heat flux anomalies over the northern oceans: Driving the sea surface temperature. *J. Phys. Oceanogr.,* **22,** 859–881.

——, and G. Reverdin, 1994: Monthly precipitation and evaporation variability estimated over the North Atlantic and North Pacific. *Proc. Atlantic Climate Change Program: PIs' Meeting,* Princeton, NJ, NOAA, 28–32.

Chapman, W. L., and J. E. Walsh, 1993: Recent variations of sea-ice and air temperature in high latitudes. *Bull. Amer. Meteor. Soc.,* **74,** 33–47.

Cheng, X., and T. J. Dunkerton, 1995: Orthogonal rotation of spatial patterns derived from singular value decomposition analysis. *J. Climate,* **8,** 2631–2643.

Cook, E. R., R. D. D'Arrigo, and K. R. Briffa, 1998: A reconstruction of the North Atlantic oscillation using tree-ring chronologies from North America and Europe. *Holocene,* **8,** 9–17

Cotton, P. D, and P. G. Challenor, 1999: North Atlantic wave climate variability and the North Atlantic oscillation index. *Proc. Ninth ISOPE Conf.,* Brest, France, International Society of Offshore and Polar Engineers, Vol. 3, 153–157.

Curry, R. G., M. S. McCartney, and T. M. Joyce, 1998: Oceanic transport of subpolar climate signals to mid-depth subtropical waters. *Nature,* **391,** 575–577.

Deser, C., 2000: On the teleconnectivity of the Arctic oscillation. *Geophys. Res. Lett.,* in press.

——, and M. L. Blackmon, 1993: Surface climate variations over the North Atlantic Ocean during winter: 1900–1989. *J. Climate,* **6,** 1743–1753.

——, J. E. Walsh, and M. S. Timlin, 2000: Arctic sea ice variability in the context of recent wintertime atmospheric circulation trends. *J. Climate,* **13,** 617–633.

Dickson, R. R., 1997: From the Labrador Sea to global change. *Nature,* **386,** 649–650.

——, 1999: All change in the Arctic. *Nature,* **397,** 389–391.

——, and J. Namias, 1976: North American influences on the circulation and climate of the North Atlantic sector. *Mon. Wea. Rev.,* **104,** 1256–1265.

——, and J. Blindheim, 1984: On the abnormal hydrographic conditions in the European Arctic during the 1970s. *Rapp. P.-V. Reun. Cons. Int. Explor. Mer,* **185,** 201–213.

——, and W. R. Turrell, 1999: The NAO: The dominant atmospheric process affecting oceanic variability in home, middle and distant waters of European salmon. *The Ocean Life of Atlantic Salmon,* D. Mills, Ed., Fishing News Books, 92–115.

——, J. Meincke, S.-A. Malmberg, and A. J. Lee, 1988: The ''Great Salinity Anomaly'' in the northern North Atlantic 1968–1982. *Progress in Oceanography,* Vol. 20, Pergamon Press, 103–151.

——, J. Lazier, J. Meinke, P. Rhines, and J. Swift, 1996: Long-term coordinated changes in the convective activity of the North Atlantic. *Progress in Oceanography,* Vol. 38, Pergamon Press, 241–295.

——, J. Meincke, I. M. Vassie, J. Jungclaus, and S. Osterhus, 1999: Possible predictability in overflow from the Denmark Strait. *Nature,* **397,** 243–246.

Environmental Working Group, 1997: *Joint US-Russian Atlas of the Arctic Ocean; Oceanography Atlas for the Winter Season.* National Snow and Ice Data Center, CD-ROM.

Fang, Z., and J. M. Wallace, 1994: Arctic sea-ice variability on a time-scale of weeks and its relation to atmospheric forcing. *J. Climate,* **7,** 1897–1914.

Friedland, K. D., D. G. Reddin, and J. F. Kocik, 1993: Marine survival of North American and European Atlantic salmon: Effects of growth and environment. *ICES J. Mar. Sci.,* **50,** 481–492.

Fromentin, J.-M., and B. Planque, 1996: Calanus and environment in the eastern North Atlantic. Part II: Influence of the North Atlantic oscillation on *C. finmarchicus* and *C. helgolandicus. Mar. Ecol. Prog. Ser.,* **134,** 111–118.

Grotefendt, K., K. Logemann, D. Quadfasel, and S. Ronski, 1998: Is the Arctic Ocean warming? *J. Geophys. Res.,* **103,** 27 679–27 687

Hansen, D. V., and H. F. Bezdek, 1996: On the nature of decadal anomalies in the North Atlantic sea surface temperature. *J. Geophys. Res.,* **101,** 9749–9758.

Harder, M., P. Lemke, and M. Hilmer, 1998: Simulation of sea-ice transport through Fram Strait: Natural variability and sensitivity to atmospheric forcing. *J. Geophys. Res.,* **103,** 5595–5606.

Helland-Hansen, B., and F. Nansen, 1909: The Norwegian Sea. *Fiskeridir. Skr. Ser. Havunders.,* **2,** 1–360.

Houghton, R. W., 1996: Subsurface quasi-decadal fluctuations in the North Atlantic. *J. Climate,* **9,** 1363–1373.

Hurrell, J. W., 1995a: Decadal trends in the North Atlantic oscillation: Regional temperatures and precipitation. *Science,* **269,** 676–679.

——, 1995b: An evaluation of the transient eddy forced vorticity balance during northern winter. *J. Atmos Sci.,* **52,** 2286–2301.

——, 1996: Influence of variations in extratropical wintertime teleconnections on Northern Hemisphere temperature. *Geophys. Res. Lett.,* **23,** 665–668.

——, and H. van Loon, 1997: Decadal variations in climate associated with the North Atlantic oscillation. *Climatic Change,* **36,** 301–326.

ICES, 1996: Report of the Cod and Climate Backward-Facing Workshop, Bergen. ICES CM, Mimeo 1996/A:9, 20 pp. [Available from ICES Secretariat, Palaegade 2–4, DK-1261, Copenhagen-K Denmark.]

Johannessen, O. M., M. Miles, and E. Bjorgo, 1995: The Arctic's shrinking sea ice. *Nature,* **376,** 126–127.

Jones, P. D., 1987: The early twentieth century Arctic high—Fact or fiction? *Climate Dyn.,* **1,** 63–75.

——, T. Jonsson, and D. Wheeler, 1997: Extension of the North Atlantic oscillation using early instrumental pressure observations from Gibraltar and south-west Iceland. *Int. J. Climatol.,* **17,** 1433–1450.

Joyce, T. M., and P. Robbins, 1996: The long-term hydrographic record at Bermuda. *J. Climate,* **9,** 3121–3131.

——, R. S. Pickart, and R. C. Millard, 1999: Long-term hydrographic changes at 52° and 66°W in the North Atlantic Subtropical Gyre and Caribbean. *Deep-Sea Res. II,* **46,** 245–278.

——, C. Deser, and M. A. Spall, 2000: The relation between decadal

variability of subtropical mode water and the North Atlantic oscillation. *J. Climate,* **13,** 2250–2569.
Kahl, J. D., S. Shiotani, S. M. Skony, and R. C. Schell, 1992: In situ meteorological sounding archives for Arctic studies. *Bull. Amer. Meteor. Soc.,* **73,** 1824–1830.
Kitoh, A., H. Doide, K. Kodera, S. Yukimoto, and A. Noda, 1996: Interannual variability in the stratospheric–tropospheric circulation in a coupled ocean–atmosphere GCM. *Geophys. Res. Lett.,* **23,** 543–546.
Kodera, K., M. Chiba, H. Koide, A. Kitoh, and Y. Nikaidou, 1996: Interannual variability of the winter stratosphere and troposphere in the Northern Hemisphere. *J. Meteor. Soc. Japan,* **74,** 365–382.
Kolatschek, J., H. Eicken, V. Yu. Alexandrov, and M. Kreyscher, 1996: The sea-ice cover of the Arctic Ocean and the Eurasian marginal seas: A brief overview of present day patterns and variability. Berichte zur Polarforschung 212, Alfred-Wegener Institut für Polar und Meeresforschung, Bremerhaven, Germany, 324 pp. [Available from A-W-I, Columbusstrasse, D-27568, Bremerhaven, Germany.]
Kushnir, Y., V. J. Cardone, J. G. Greenwood, and M. Cane, 1997: On the recent increase in North Atlantic wave heights. *J. Climate,* **10,** 2107–2113.
Kwok, R., and D. A. Rothrock, 1999: Variability of Fram Strait ice flux and the North Atlantic oscillation. *J. Geophys. Res. Oceans,* **104,** 5177–5189.
Lazier, J. R. N., 1995: The salinity decrease in the Labrador Sea over the past thirty years. *Natural Climate Variability on Decade-to-Century Time Scales,* D. G. Martinson et al., Eds., National Academy Press, 295–304.
Loeng, H., V. Ozhigin, and B. Adlandsvik, 1997: Water fluxes through the Barents Sea. *ICES J. Mar. Sci.,* **54,** 310–317.
Manabe, S., and R. J. Stouffer, 1993: Century-scale effects of increased atmospheric CO_2 on the ocean–atmosphere system. *Nature,* **364,** 215–218.
——, and ——, 1994: Multiple-century response of a coupled ocean–atmosphere model to an increase of atmospheric carbon dioxide. *J. Climate,* **7,** 5–23.
Mandel, S. Z., 1976: The water level in Barentsberg as an indicator of the inflow of Atlantic waters into the Arctic basin. *Proc. AANII,* **319,** 129–136.
——, 1978: Concerning the seasonal and year-to-year variations of the heat flow of Atlantic waters into the Arctic basin. *Proc. AANII,* **349,** 50–54.
——, 1979: Basic features of seasonal and year-to-year variations of the inflow of Atlantic water and of heat into the Arctic Basin through Fram Strait. *Proc. AANII,* **361,** 24–29.
Marsh, R., B. Petrie, C. R. Weidman, R. R. Dickson, J. W. Loder, C. G. Hannah, K. Frank, and K. Drinkwater, 1999: The 1882 tilefish kill—A cold event in shelf waters off the north-eastern United States? *Fish. Oceanogr.,* **8,** 39–49.
Maslanik, J. A., M. C. Serreze, and R. G. Barry, 1996: Recent decreases in Arctic summer ice cover and linkages to atmospheric circulation anomalies. *Geophys. Res. Lett.,* **23,** 1677–1680.
McCartney, M. S., R. G. Curry, and H. F. Bezdek, 1996: North Atlantic's transformation pipeline chills and redistributes subtropical water. *Oceanus,* **39,** 19–23.
——, ——, and ——, 1997: The interdecadal warming and cooling of Labrador Sea Water. *ACCP Notes,* **4,** 1–11.
McLaughlin, F. A., E. C. Carmack, R. W. Macdonald, and J. K. B. Bishop, 1996: Physical and geochemical properties across the Atlantic/Pacific water mass front in the southern Canadian Basin. *J. Geophys. Res.,* **101,** 1183–1197.
Molinari, R. L., D. Mayer, J. Festa, and H. Bezdek, 1997: Multi-year variability in the near-surface temperature structure of the midlatitude western North Atlantic Ocean. *J. Geophys. Res.,* **102,** 1183–1197.
Morison, J., M. Steele, and R. Anderson, 1998a: Hydrography of the upper Arctic Ocean measured from the nuclear submarine, USS *Pargo. Deep-Sea Res. I,* **45,** 15–38.
——, K. Aagaard, and M. Steele, 1998b: Report on the study of the Arctic Change Workshop. ARCSS Rep. 8, University of Washington, 63 pp. [Available from Polar Science Center, Applied Physics Laboratory, University of Washington, Seattle, WA 98105.]
——, ——, and ——, 2000: Recent changes in the Arctic: A review. *Arctic,* in press.
Myers, R. A., J. Helbig, and D. Holland, 1989: Seasonal and interannual variability of the Labrador Current and West Greenland Current. ICES CM Mimeo 1989/C:16, 18 pp. [Available from ICES Secretariat, Palaegade 2–4, DK-1261, Copenhagen-K Denmark.]
Mysak, L. A., R. G. Ingram, J. Wang, and A. van der Baaren, 1996: The anomalous sea-ice extent in Hudson Bay, Baffin Bay and the Labrador Sea during three simultaneous NAO and ENSO episodes. *Atmos.–Ocean,* **34,** 313–343.
Osborn, T. J., K. R. Briffa, S. F. B. Tett, P. D. Jones, and R. Trigo, 2000: Evaluation of the North Atlantic oscillation as simulated by a coupled climate model. *Climate Dyn.,* **15,** 685–702.
Parkinson, C. L., 1992: Spatial patterns of increases and decreases in the length of the sea-ice season. *J. Geophys. Res.,* **97,** 14 377–14 388.
Perlwitz, J., and H.-F. Graf, 1995: The statistical connection between tropospheric and stratospheric circulation of the Northern Hemisphere in winter. *J. Climate,* **8,** 2281–2295.
Piexoto, J. P., and A. H. Oort, 1992: *Physics of Climate.* American Institute of Physics, 520 pp.
Planque, B., and C. J. Fox, 1998: Interannual variability in temperature and the recruitment of Irish Sea cod. *Mar. Ecol. Prog. Ser.,* **172,** 101–105.
Quadfasel, D., A. Sy, D. Wells, and A. Tunik, 1991: Warming in the Arctic. *Nature,* **350,** 385.
Rahmstorf, S., and A. Ganopolski, 1999: Long-term global warming scenarios computed with an efficient coupled climate model. *Climatic Change,* **43,** 353–367.
Rhines, P., 1994: Climate change in the Labrador Sea, its convection and circulation. *Proc. Atlantic Climate Change Program: PIs' Meeting,* Princeton, NJ, NOAA, 85–96.
Rogers, J. C., 1990: Patterns of low-frequency monthly sea level pressure variability (1899–1986) and associated wave cyclone frequencies. *J. Climate,* **3,** 1364–1379.
——, 1994: Atlantic storm track variability and the North Atlantic oscillation. *Proc. Atlantic Climate Change Program*: *PIs' Meeting,* Princeton, NJ, NOAA, 20–24.
——, 1997: North Atlantic storm track variability and its association to the North Atlantic oscillation and climate variability of northern Europe. *J. Climate,* **10,** 1635–1647.
——, and E. Mosley-Thompson, 1995: Atlantic Arctic cyclones and the mild Siberian winters of the 1980s. *Geophys. Res. Lett.,* **22,** 799–802.
Serreze, M. C., J. A. Maslanik, R. G. Barry, and T. L. Demaria, 1992: Winter atmospheric circulation in the Arctic Basin and possible relationships to the Great Salinity Anomaly in the northern North Atlantic. *Geophys. Res. Lett.,* **19,** 293–296.
——, ——, J. R. Key, R. F. Kokaly, and D. A. Robinson, 1995a: Diagnosis of the record minimum in Arctic sea-ice area during 1990 and associated snow cover extremes. *Geophys. Res. Lett.,* **22,** 2183–2186.
——, M. C. Rehder, R. G. Barry, J. E. Walsh, and D. A. Robinson, 1995b: Variations in aerologically-derived Arctic precipitation and snowfall. *Ann. Glaciol.,* **21,** 77–82.
——, R. G. Barry, and J. E. Walsh, 1995c: Atmospheric water vapor characteristics at 70°N. *J. Climate,* **8,** 719–731.
——, F. Carse, R. G. Barry, and J. C. Rogers, 1997: Icelandic Low cyclone activity: Climatological features, linkages with the NAO, and relationships with recent changes in the Northern Hemisphere circulation. *J. Climate,* **10,** 453–464.
Steele, M., and T. Boyd, 1998: Retreat of the cold halocline layer in the Arctic Ocean. *J. Geophys. Res.,* **103,** 10 419–10 435.
Swift, J. H., E. P. Jones, K. Aagaard, E. C. Carmack, M. Hingston,

R. W. Macdonald, F. A. McLaughlin, and R. G. Perkin, 1997: Waters of the Makarov and Canada Basins. *Deep-Sea Res.*, **44,** 1503–1529.

Sy, A., M. Rhein, J. R. N. Lazier, K.-P. Koltermann, J. Meincke, A. Putzka, and M. Bersch, 1997: Surprisingly rapid spreading of newly formed intermediate waters across the North Atlantic Ocean. *Nature*, **386,** 675–679.

Talley, L. D., 1996: North Atlantic circulation and variability, reviewed for the CNLS Conference, Los Alamos, May 1995. *Physica D,* **98,** 625–646.

Tereshchenko, V. V., 1996: Seasonal and year-to-year variations of temperature and salinity along the Kola meridian transect. ICES CM Mimeo 1996/C:11, 24 pp. [Available from ICES Secretariat, Palaegade 2–4, DK-1261, Copenhagen-K Denmark.]

Thompson, D. W. J., and J. M. Wallace, 1998: The Arctic oscillation signature in the wintertime geopotential height and temperature fields. *Geophys. Res. Lett.*, **25,** 1297–1300.

——, and ——, 2000: Annular modes in the extratropical circulation. Part I: Month-to-month variability. *J. Climate,* **13,** 1000–1016.

——, ——, and G. C. Hegerl, 2000: Annular modes in the extratropical circulation. Part II: Trends. *J. Climate,* **13,** 1018–1036.

Trenberth, K. E., and D. A. Paolino, 1980: The Northern Hemisphere sea-level pressure data set: Trends, errors and discontinuities. *Mon. Wea. Rev.,* **108,** 855–872.

——, and J. W. Hurrell, 1994: Decadal atmosphere–ocean variations in the Pacific. *Climate Dyn.,* **9,** 303–319.

Vinje, T., 1998: On the variation during the past 400 years of the Barents Sea ice edge position and Northern Hemisphere temperatures. *Proc. WCRP Symp. on Polar Processes and Global Climate,* Rosario, Orcas Island, WA, WCRP, 271–273.

——, and O. Finnekasa, 1986: The ice transport through the Fram Strait. *Norsk Polarinst. Skr.,* **186,** 37–39.

——, N. Nordlund, and A. Kvambekk, 1998: Monitoring ice thickness in Fram Strait. *J. Geophys. Res.,* **103,** 10 437–10 449.

Walsh, J. E., W. L. Chapman, and T. L. Shy, 1996: Recent decrease of sea level pressure in the central Arctic. *J. Climate,* **9,** 480–486.

WASA Group, 1997: Changing waves and storms in the northeast Atlantic? GKSS Forschungszentrum Geesthacht GmbH Rep. 97/E/46, 23 pp. [Available from GKSS-Forschungszentrum, Geesthacht GmbH, Library, Postfach 1160, D-21494, Geesthacht, Germany.]

WMO, 1994: WCRP-5 initial implementation plan for the Arctic Climate System Study (ACSYS). WMO/TD 627, World Meteorological Organization, 66 pp.

Xie, P., and P. A. Arkin, 1996: Analyses of global monthly precipitation using gauge observations, satellite estimates and numerical model prediction. *J. Climate,* **9,** 840–858.

Zakharov, V. F., 1976: Cooling of the Arctic and ice cover in the Arctic seas. *Trudi AANI,* **337,** 95 pp.

Zhang, Y., W. Maslowski, and A. J. Semtner, 1999: Impacts of mesoscale ocean currents on sea ice in high resolution Arctic ice and ocean simulations. *J. Geophys. Res.,* **104,** 18 409–18 429.